Copy _____

IDA DOCUMENT D-1816

THE LOWEST ATMOSPHERE: ATMOSPHERIC BOUNDARY LAYER INCLUDING ATMOSPHERIC SURFACE LAYER

Ernest Bauer

April 1996

Prepared for
Defense Advanced Research Projects Agency

INSTITUTE FOR DEFENSE ANALYSES
1801 N. Beauregard Street, Alexandria, Virginia 22311-1772

IDA Log No. H 95-47561

DISCLAIMER NOTICE

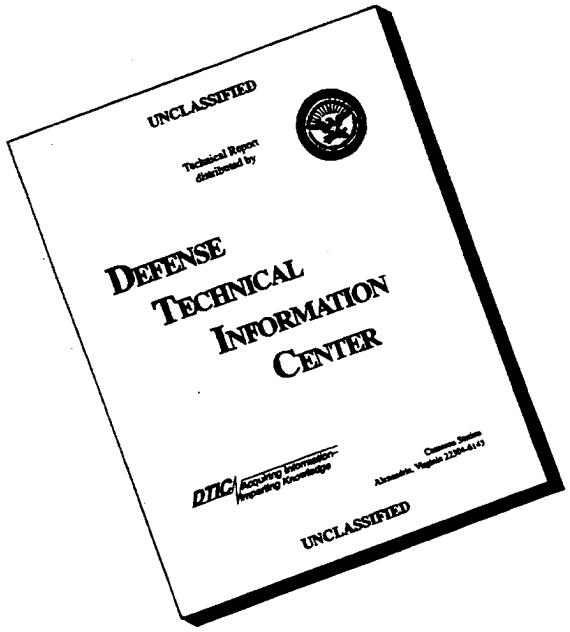

THIS DOCUMENT IS BEST QUALITY AVAILABLE. THE COPY FURNISHED TO DTIC CONTAINED A SIGNIFICANT NUMBER OF PAGES WHICH DO NOT REPRODUCE LEGIBLY.

The work was conducted under contract DASW01 94 C 0054 for the Defense Advanced Research Projects Agency. The publication of this IDA document does not indicate endorsement by the Department of Defense, nor should the contents be construed as reflecting the official position of that Agency.

IDA DOCUMENT D-1816

THE LOWEST ATMOSPHERE: ATMOSPHERIC BOUNDARY LAYER INCLUDING ATMOSPHERIC SURFACE LAYER

Ernest Bauer

April 1996

INSTITUTE FOR DEFENSE ANALYSES
Contract DASW01 94 C 0054
DARPA Assignment A-180

PREFACE

This document was prepared in partial fulfillment of a task on Clutter Characterization and Modeling.

PROLOGUE

The lowest portion of the atmosphere, or the *Atmospheric Boundary Layer* (ABL), is affected very much by the properties of the Earth's (land or ocean) surface and may show a large diurnal variation in wind, temperature, and stability. The ABL is typically 0.5–1 km deep, representing perhaps 10 percent of the total mass of the atmosphere. The lowest 10 percent (50–150 m), the *Atmospheric Surface Layer* (ASL), is the region we live in and some of its characteristics are of considerable importance for a variety of applications.

This document began with a manuscript of April 1975 on the Planetary Boundary Layer and has grown to include the basic physics background for a variety of applications, such as the spreading of tracer clouds in the atmosphere, forest fires, and optical refraction near the surface (mirages). Note that the concept of an ABL was not frequently introduced in meteorology textbooks of the 1960's and 1970's. It is now becoming customary to use the terms Atmospheric (vs. Planetary) Boundary Layer and Atmospheric Surface Layer to distinguish them from the comparable Oceanic Layers.

Note that the top of the ABL is normally placed at 0.5–1 km, which is appropriate for midlatitude conditions. However, at some low-latitude locations such as the Persian Gulf or central Texas the top of the ABL frequently reaches 3–4 km in the daytime in summer.

CONTENTS

FIGURES

TABLES

1.0 INTRODUCTION AND SUMMARY

1.1 BACKGROUND

In a broad sense, the atmosphere as a whole may be regarded as an atmospheric boundary layer for the Earth moving in space, with a relatively high density of gaseous material (air, density ~ 1 kg/m^3 at sea level), which gravitational forces hold close (e-folding distance H = kT/Mg ~ 7 km) to the solid or liquid surface and to sub-surface material of density 1,000–3,000 kg/m^3.

The "boundary layer" is that region in which the (horizontal) wind goes from zero along the surface of the Earth to the geostrophic value $\mathbf{v}_g$[1] (discussed in Section 2.1 or Section 3) in the "free troposphere" as a result of frictional forces. A good definition of the atmospheric boundary layer (ABL) (provided to me by the late Dr. Rudy Penndorf) is:

> A layer in which a noticeable influence of the Earth's surface on wind occurs by friction. The upper boundary is determined by the altitude at which the wind vector is approximately equal to the geostrophic or gradient wind. Within the ABL, the wind direction and speed are affected by friction near the ground in establishing the "Ekman spiral" (see Section 3.3). The upper boundary of the ABL is frequently, but not always, characterized by a temperature inversion.
>
> Clouds are missing in the ABL, but haze or mist may form. There is a lot of turbulence in this layer due to heating of the ground, and adiabatic or even stronger (super-adiabatic) temperature gradients may result in the ABL from radiative processes involving the ground. If the inversion is strong, it blocks mixing with air from above.

1.2 SUMMARY

For orientation, Fig. 1 shows the temperature structure of the Earth's atmosphere over land, including the various sources of energy from the sun:

(a) Heating of the ground by incident solar radiation, which immediately warms the ABL after sunrise and so affects the rest of the atmosphere.

---

[1] Above the ABL, where immediate effects of surface irregularity are no longer important, the balance between the *pressure gradient force* and the *centrifugal force due to the rotation of the earth* (the *Coriolis force*) gives the *geostrophic wind.*

(b) Photodissociation of ozone (O_3) by UV-B (230–300 nm, i.e., a fraction of about 1 percent of the solar irradiance), which heats the stratosphere in the 30–50 km altitude range.

(c) Photoexcitation and photodissociation of oxygen (O_2) by VUV (vacuum ultraviolet) with wavelengths above roughly 150 nm, a fraction of order 10^{-3} of the solar irradiance, which heats the very tenuous upper atmosphere, the "thermosphere" in the (100^+) km altitude range.

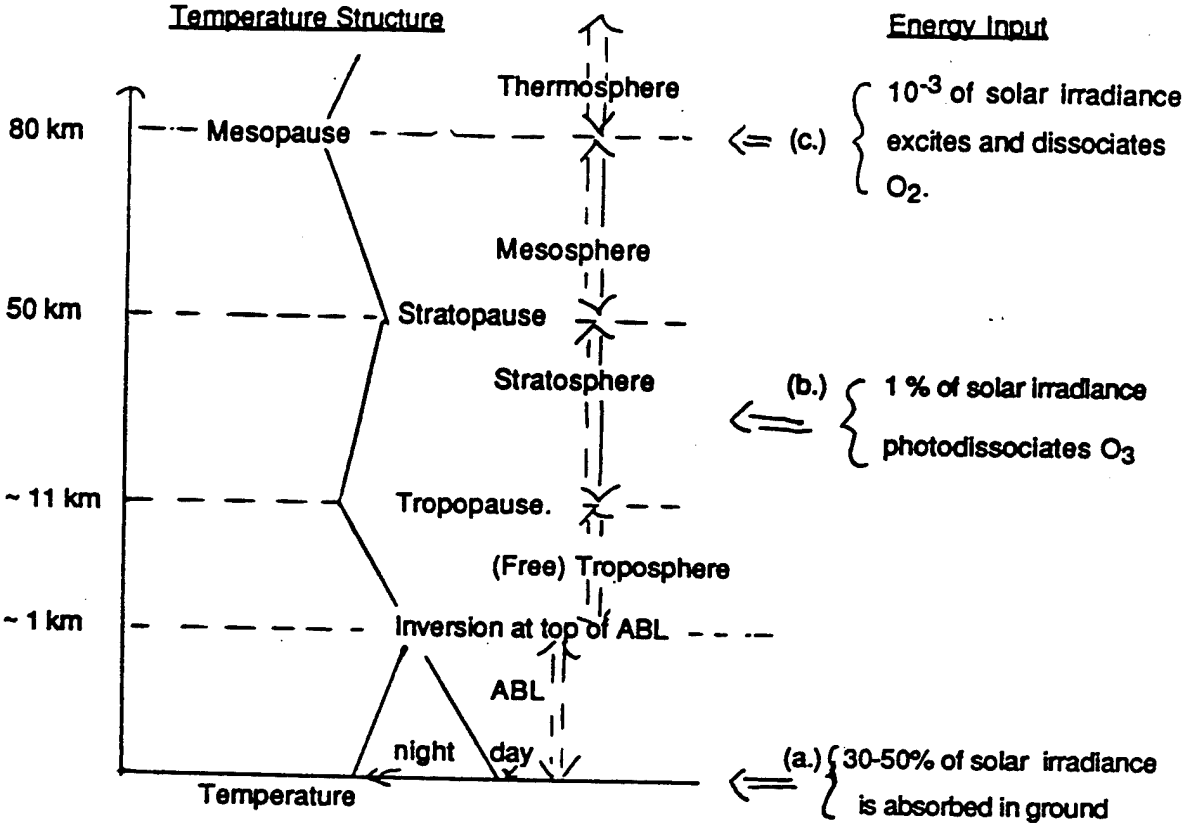

Figure 1. Vertical Structure of the Atmosphere Over Land: Schematic

Figure 2 shows the structure of the ABL over land, indicating in an overall way both the day-night temperature variation over land and how the ABL provides a connection between the ground and the free troposphere (and upper atmosphere).

The ABL represents roughly 10 percent of the atmospheric mass; the strong diurnal temperature variability shown in Figs. 1 and 2 applies only over land, not over water, because the large heat capacity of the ocean means that day-night temperature differences over water are perhaps 0.1 °C, as compared with 10–15 °C over land. Since roughly two-thirds of the Earth is covered with water, this is indeed an important caveat; Section 2.3 discusses the ABL over land, and Section 2.5 discusses the ABL over the

ocean. Much of the diurnal variation over land takes place in the lowest 100 meters above the surface, in the *atmospheric surface layer* (ASL), which is roughly the lowest 10 percent of the ABL or 1 percent of the total atmosphere. Thus attention is now increasingly being directed towards the ASL (discussed in Section 2.4).

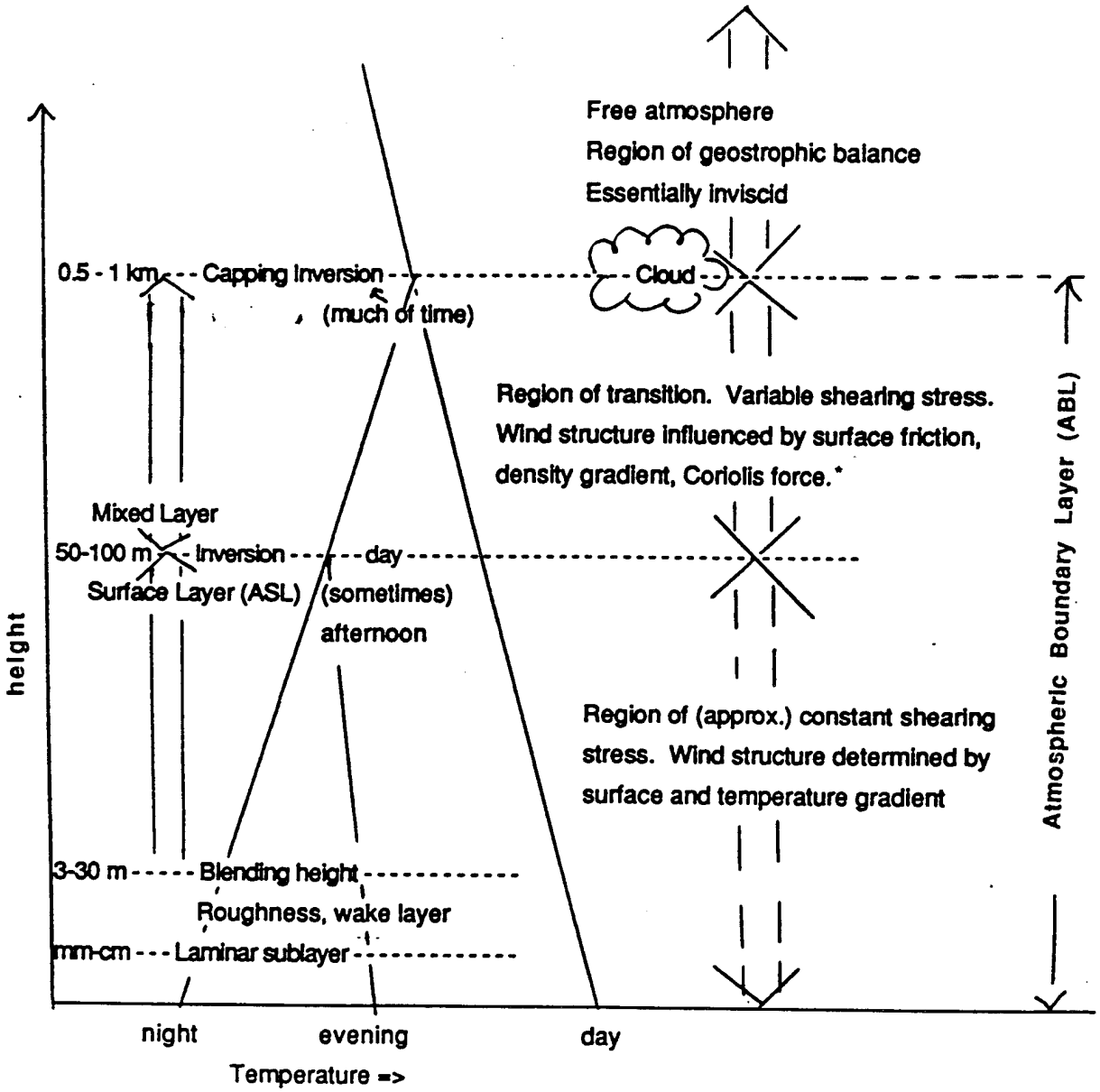

* Coriolis force is the centrifugal force due to the rotation of the Earth.

Figure 2. Structure of the ABL Over Land: Schematic

1.3 OUTLINE

The structure of this document is the following. The main problem in the ABL is the interaction between the surface (land and ocean) and the atmosphere, and the key parameters are wind, the vertical temperature/stability profile and turbulence. Section 2 begins with a discussion of the scales of atmospheric motions and the wind and its variation, including the commonly used Beaufort scale of wind force (see Table 2 below). Section 2.3 reviews atmospheric variability, and Section 2.4 treats the structure of the ABL over land; the atmospheric surface layer (ASL), the lowest 10 percent of the ABL, is reviewed in Section 2.5. The ABL over the ocean is reviewed in Section 2.6, and Section 2.7 finishes with an overview of the interaction between the atmosphere and the underlying Earth or ocean surface.

Section 3 discusses winds, beginning with the geostrophic wind v_g, the mean horizontal wind above the ABL whose value provides one boundary condition for the wind field in the ABL; the second one is the condition of zero slip along the surface. Near the equator where the Coriolis parameter[2] is very small, the geostrophic wind and the ABL are not well defined: see Section 3.5 for a brief discussion of what happens to the ABL in the equatorial region. Section 4, "In Closing," does just that, pointing out that the study of the ABL has been of very recent origin, referring the reader largely to specific articles in technical encyclopedias which treat the problems at what I consider a useful level, emphasizing the physics rather than quantitative details, so that one does not miss an overview of the forest by studying details of the trees.

Appendix A supplements Section 2.3 by expanding on the important meteorological concept of atmospheric stability. This is frequently discussed in terms of the height variation of the *potential temperature* $\theta = T(p_o/p)^{R/Cp}$, which is introduced in Section 2.3 and discussed in Appendix A.

---

[2] $f = 2\,\Omega \sin\phi$ where Ω = angular velocity of rotation of the earth and ϕ = latitude; see Sections 2.1 and 3.2.

2.0 TEMPERATURE STRUCTURE, WIND, AND TURBULENCE IN THE ABL: SURFACE LAYER AND MIXED REGION

2.1 WIND FIELD IN THE LOWER ATMOSPHERE

The atmospheric velocity $\mathbf{v}(\mathbf{x},t)$ varies both with space and time on a wide variety of scales. It is frequently convenient to split this into two components by averaging over time (with an averaging time of order minutes):

$$\mathbf{v}(\mathbf{x},t) = \mathbf{v}_{\mathbf{av}}(\mathbf{x},t) + \mathbf{v}'(\mathbf{x},t) \quad . \tag{1}$$

Here $\mathbf{v}_{\mathbf{av}}(\mathbf{x},t)$ is the mean wind and the time average of the fluctuation $\mathbf{v}'(\mathbf{x},t)$ is zero.

Equation (1) is a formal representation of the very complex time variation of the wind in the Earth's atmosphere; Section 2.2 presents an overview of what "truly" goes on.

The second term in Equation (1), $\mathbf{v}'(x,t)$, represents atmospheric turbulence, which is very important for the mixing and dispersion of impurities or tracers in the atmosphere. Atmospheric turbulence is due to the combined effects of heat turbulence (convection) and mechanical turbulence (wind shear). The centrifugal force on an air parcel due to the rotation of the Earth (Coriolis effect) is important for many problems in large-scale atmospheric motions.

On account of gravity, the mean wind is essentially horizontal; typically the horizontal wind speed is ~10 m/sec, while the vertical wind speed is ~ 1–10 cm/sec (see Section 3). At the top of the ABL the mean wind is roughly equal to the geostrophic wind $\mathbf{v}_g$; the transition depends on the nature of the surface (see, e.g., Fig. 11 and Sections 3.2–3.4). The geostrophic wind $\mathbf{v}_g$ is given by the balance between the Coriolis force, which is the centrifugal force on an air parcel arising from the rotation of the Earth, and the horizontal component of the atmospheric pressure gradient

$$\mathbf{v}_g = (1/\rho\, f)\, [\mathbf{k} \times \mathrm{grad}_H\, p] \quad , \tag{2}$$

where ρ = atmospheric density

$f = 2\,\pi\,\Omega \sin\phi$, the Coriolis parameter at latitude ϕ

Ω = 7.29×10^{-5} radian sec^{-1}, the rotation rate of the Earth

k = unit spatial vector in the vertical (z) direction

$grad_H$ = horizontal component of the (spatial) gradient

p = pressure

$[\mathbf{A} \times \mathbf{B}]$ = vector (cross) product of **A** and **B.**

For many applications, one characterizes atmospheric motions as one of the following three situations:

- Unstable: here there is convective overturning, typical of fine sunny afternoons with relatively low wind, when there may be cumulus clouds.
- Stable: low wind and low convection, typical of a clear night.
- Neutral: intermediate conditions, typically a grey day with (stratiform) cloud cover and relatively high wind.

The concept of atmospheric stability is discussed in some detail in Section 2.3, and expanded in Appendix A.

Note that low wind-speed conditions are particularly significant for air pollution, because this is when the emitted materials simply accumulate, leading to greatly enhanced levels of pollutants and thus severely degraded air quality.

1. The standard instrument used for measuring wind speed, the anemometer, does not register well for wind speeds below about 2 m/sec,[3] which occur (in the UK) some 10–30 percent of the time.
2. The standard models of atmospheric stability, which are discussed in Section 2.3, tend to fail for wind speeds below ~ 2 m/sec (4 mph).
3. When the wind speed is low, *topographic control*, or the influence of irregular land surfaces such as slopes, hills, valleys and coastlines, is more important than *geostrophic control*, or the motion of the free atmosphere. Indeed, the ABL is defined as that region of the atmosphere in which the influences of the surface are important; thus the height of the ABL ranges from perhaps 300 m under high-wind conditions to 3–4 km under extreme thermal control (e.g., in low-latitude deserts under maximum insolation, such as at 1,200–1,400 LT in summer in Central Texas or in the Arabian Gulf).

[3] Anemometers are designed to perform reliably at high wind speeds, say > 10 m/sec or 20 mph.

Some of the phenomena associated with topographic control include:

- Land-breezes and sea-breezes
- Mountain and valley winds, including mountain waves

See, e.g., McIlveen (1992, Ch. 9) for a discussion of the surface microclimate including effects such as fog, which is affected largely by ground cover[4] (also Geiger, 1965; Oke, 1978).

2.2 ATMOSPHERIC/WIND VARIABILITY

The motion of the atmosphere varies on all scales of space and time, ranging from centimeters and seconds to a global scale (24,000 km) and years. Depending on how one chooses to look at this variability, a variety of descriptions of the motion can be given.

- For an overview of air motions in the ABL with particular reference to the Former Soviet Union, see Tverskoi (1965, esp. Ch. 23).
- A simple conceptual division is to describe the wind $\mathbf{v}(\mathbf{x},t)$ by Eq. (1), where $\mathbf{v}_{av}(\mathbf{x},t)$ is the mean wind (averaged over some seconds to a few minutes in an anemometer measurement) and $\mathbf{v}'(\mathbf{x},t)$ is its spatial-temporal fluctuation, called "turbulence."
- Atmospheric turbulence is a complex phenomenon, ascribed to the effects of a combination of wind shear and thermal gradients (see, e.g., McIlveen, 1992, p. 303 ff.; Panofsky and Dutton, 1984; or Panofsky, 1992).
- Meteorologists divide the motion into different space-time ranges as indicated in Table 1.
- Fluid mechanicians analyze the elastic motions of the air in terms of different restoring forces, either compressibility or gravity. In this way there are two principal elastic modes, namely high-frequency infrasonic waves and low-frequency[5] internal gravity or buoyancy waves (see Gossard and Hooke, 1975).
- In the days of wind-powered sailing ships, sailors needed an empirical description of the varying wind force, and a useful one was provided in 1805 by the British Admiral Beaufort. It has been generalized to terrestrial as well as maritime conditions and is given as Table 2; because the descriptors are different over land and over water, we show two distinct versions of the table.

---

4 A striking effect is radiation fog which occurs over open fields in the morning when radiative heat loss to space (in the absence of clouds) has cooled the air below the dew point; by contrast, inside neighboring forests the air is clear, because the tree cover has reduced cooling sufficiently so that the temperature under the trees remains above the local dew point.

5 Period greater than the Brunt-Vaisala period N ~ 2 minutes.

Table 1. Scales of Atmospheric Motions

Region of Fig.*	Scale	Phenomena	Affected Scale (Approximate)	
			Horizontal Dimension	Time
From Hobbs (1981): Different Atmospheric Motions				
H1	Micro-γ δ	Plumes, Mechanical and Isotropic Turbulence	2 mm to 20 m	1 sec to 1 min
H2	Micro-β	Dust Devils, Thermals, Wakes	20 m to 200 m	0.5 min to 3 min
H3	Micro-α	Tornadoes, Deep Convection, Short Gravity Waves	200 m to 2 km	2 min to 1 hr
H4	Meso-γ	Thunderstorms, Internal Gravity Waves, Clear Air Turbulence, Urban Effects	2 to 20 km	6 min to 3 hr
H5	Meso-β	Nocturnal Low-Level Jet, Inertial Waves, Cloud Clusters, Mountain and Lake Disturbances, Rainbands, Squall Lines	20 to 200 km	2 hr to 1 day
H6	Meso-α	Front Hurricanes	200 m to 2,000 km	5 days to 1 month
H7	Macro-β	Baroclinic Waves	2,000 km to 5,000 km	2 days to 1 month
H8	Macro-α	Standing Waves, Ultra-long Waves, Tidal Waves	> 10,000 km	> 1 day
From Ramage (1976): Turbulence Bursts on Different Scales				
R1	Convective	Hot Towers	2 km to 10 km	15 min to 2 hr
R2	Mesoscale	Flash Floods	10 km to 100 km	2 hr to 6 hr
R3	Sub-synoptic	Tornadoes, Clear Air Turbulence, etc.	100 km to 500 km	6 hr to 12 hr
R4	Synoptic	Continuous Thunderstorms, Large Scale Convection	500 km to 2,000 km	12 hr to 48 hr
R5	Planetary	Hurricanes, etc.	> 2,000 km	24 hr to 48 hr

* The regions H1–H8 and R1–R5 are defined in Figure 5, below.

Table 2a. Beaufort Scale of Wind Force Over Land

Force	Wind Speed (km/hr)	Description	Effects
0	< 1	Calm	Calm. Smoke rises vertically.
1	1–5	Light air	Direction of wind shown by smoke drift, not by vane.
2	6–11	Light breeze	Wind felt on face; leaves rustle; ordinary vane moved by wind.
3	12–19	Gentle breeze	Leaves and small twigs in constant motion; wind extends light flag.
4	20–28	Moderate	Raises dust and loose paper; small branches are moved.
5	29–38	Fresh	Small trees in leaf begin to sway; crested wavelets form on inland waters.
6	39–49	Strong	Large branches in motion; whistling heard in telegraph wires; umbrellas used with difficulty.
7	50–61	Moderate gale	Whole trees in motion; inconvenience felt when walking against wind.
8	62–74	Gale	Breaks twigs off trees; generally impedes progress.
9	75–88	Strong gale	Slight structural damage occurs; chimney pots and slates removed.
10	89–102	Whole gale	Seldom experienced inland; trees uprooted; considerable structural damage occurs.
11	103–114	Violent storm	Rarely experienced; widespread damage occurs.
12	115 and above	Hurricane	Rare inland; severe and widespread damage, flooding, etc.

Table 2b. Beaufort Scale of Wind Force Over the Ocean

Force	Wind Speed (km/hr)	Average Wave Height (m)	Description	Effects
0	< 1	0	Calm	Calm. Sea like a mirror.
1	1–5	0	Light air	Ripples like scales, no foam crest.
2	6–11	0–0.3	Light breeze	Small wavelets; crests have glassy appearance, do not break.
3	12–19	0.3–0.6	Gentle breeze	Large wavelets; crests begin to break; foam looks glassy.
4	20–28	0.6–1.2	Moderate breeze	Small waves becoming longer; some white horses.
5	29–38	1.2–2.4	Fresh breeze	Moderate waves, becoming longer; many white horses; chance of some spray.
6	39–49	2.4–4	Strong breeze	Large waves begin to form; white foam crests more extensive; probably some spray.
7	50–61	4–6	Near gale	Sea heaps up, white foam from breaking waves begins to be blown along wind direction.
8	62–74	4–6	Gale	Moderately high waves of greater length; edges of crests begin to break into spindrift; foam is blown in streaks along wind direction.
9	75–88	4–6	Strong gale	High waves; dense streaks of foam along wind direction; crests of waves begin to topple, tumble, and roll over; spray may affect visibility.
10	89–102	6–9	Storm/ Whole gale	Very high waves with long over-hanging crests; great patches of foam blown in dense white streaks; surface of sea takes a white appearance; tumbling of sea becomes heavy and shock-like; visibility affected.
11	103–114	9–14	Violent storm	Exceptionally high waves; small and medium-sized ships might be lost to view behind the waves; the sea is completely covered with long white patches of foam lying in wind direction; edges of wave crests are blown into froth; visibility affected.
12	115 and above	> 14	Hurricane	The air is filled with foam and spray; sea completely white with driving spray; visibility very seriously affected.

2.3 ATMOSPHERIC STABILITY: TEMPERATURE AND DENSITY PROFILES, MAINLY IN THE ATMOSPHERIC SURFACE LAYER

Let us now ask for the motion of the atmosphere, discussing first the stability of individual air parcels with respect to vertical displacements. This concept is critical for understanding atmospheric convection, which underlies the thermal component of atmospheric turbulence.[6]

We see from Fig. 2 (above) that the atmospheric temperature normally changes with height. There are two distinct cases:

1. If warm air overlies cold air, the atmosphere is *stable*, in that if an air parcel is displaced vertically it tends to return to its initial position.
2. If cold air overlies warm air, the atmosphere is *unstable*, subject to convective overturning.

For a quantitative discussion of atmospheric stability it is convenient to replace temperature T by potential temperature θ:

$$\theta = T(p_o/p)^{R/Cp} = T(p_o/p)^{0.286} \quad , \tag{3}$$

where p_o is a reference pressure normally chosen as 1,000 mb.[7] θ is conserved in the adiabatic[8] motion of an air parcel, and satisfies the conditions:

$$\partial\theta/\partial z = 0 \text{ for neutral stability} \tag{4a}$$

$$\partial\theta/\partial z < 0 \text{ for unstable conditions} \tag{4b}$$

$$\partial\theta/\partial z > 0 \text{ for stable conditions} \quad . \tag{4c}$$

These criteria determine the vertical motion in the atmosphere. In meteorology one often describes the state of a particular air parcel by the parameters θ and p rather than by T and p, because the trajectory of an air parcel on an adiabatic diagram or tephigram (with θ and p axes) makes it clear if a particular air parcel is stable or unstable (see, e.g., Fig. A-2 in Appendix A).

---

6 Stull, 1991, points out that atmospheric stability and lapse rate should be defined between two definite altitudes z_1 and z_2 and the corresponding temperatures T_1 and T_2. In other words, the details of the temperature variation between z_1 and z_2 do not matter, but the stability between z_1 and z_3 on the one hand and z_3 and z_2 on the other could be different, where z_3 lies between z_1 and z_2.

7 The standard sea level pressure is 1,013 mb.

8 An adiabatic displacement is one in which no energy is added to or taken from the air parcel: an adiabatic and reversible displacement of an air parcel is called an isentropic displacement, because entropy remains constant in a reversible adiabatic displacement.

In the surface layer the stability of the atmosphere determines the rate of dispersion of pollutant or tracer clouds. Table 3 presents a characterization of atmospheric stability in terms of the 6–7 Pasquill-Gifford stability classes A–F/G (Pasquill and Smith, 1983). This includes estimates developed (by the U.S. Environmental Protection Agency) for conditions over land in the USA: these estimates do not necessarily apply over water, or in different geographic regions.

Table 3. Classes of Atmospheric Stability (from

A. DEFINITION

Type	Characteristics	Nuclear Regulatory Commission, 1980		
		Pasquill Category	Vertical T-gradient (°C/100 m)	Horiz.wind dispersion Std. Dev. over 15 min–1 hr
Unstable	Day, Bright Sun, Convection	A–C	$\Delta T/\Delta z > -1.5$	$\sigma_\theta > 12.5°$
Neutral	Cloudy , windy	D	$-1.5 > \Delta T/\Delta z > -.5$	$12.5° > \sigma_\theta > 7.5°$
Stable	Night, low wind, little cloud	E–F/G	$-.5 > \Delta T/\Delta z > (+5)$	$\sigma_\theta > 7.5°$

B. SIMPLE CHARACTERIZATION (Source: U.S. Forest Service, 1976)

Wind speed (@ 10 m)		Day			Overcast	Night
m/sec	mph	strong sun	mod. sun	slight sun	> 4/8 cloud cover	> 3/8 cloud cover
<2	< 4.5	A	A–B	B	F	G
2–3	4.5–7	A–B	B	C	E	F
3–5	7–11	B	B–C	C	D	E
5–6	11–13.5	C	C–D	D	D	D
>6	> 13.5	C	D	D	D	D

C. RELATIVE FREQUENCY (%) at 10 U.S. Stations (Source: Doty et al., 1976)

Category:	A	B	C	D	Stable (E–G)
Summer	4.2	14.0	16.5	30.2	35.9
Winter	0.3	4.1	8.0	48.0	39.6
Annual (4 seasons)	1.8	8.6	11.6	40.2	37.7

From Table 3 it is clear that some judgment is called for in the assignment of Pasquill-Gifford classes, and indeed Panofsky and Dutton (1984, p. 244) suggest that the Pasquill-Gifford stability classes are misused in that many situations are listed as "neutral" or D stability, when B or C stability would be more appropriate. Note that:

1. Cloudy conditions are very common, occurring some 60 percent on a global average basis (cf. Mochow and Schlesinger, 1994).
2. Not everybody uses the "extremely stable" category G.
3. In many applications the 6–7 Pasquill-Gifford stability categories are replaced by just 3–5 categories, as in Fig. 4.

For cloud dispersion it is customary to consider a steady tracer source of strength Q (injectant per unit time) at effective height z = h, with a uniform steady wind of speed u blowing in the x-direction. The concentration of injected material $\chi(x,y,z;h)$ is written as

$$\chi(x,y,z;h) = Q/(2\,\pi\,\sigma_y\,\sigma_z\,u)\,\exp[-(1/2)\,(y/\sigma_y)^2]\,\{\exp[-(1/2)\,\{z-h)/\sigma_z\}^2 + R\,\exp[-(1/2)\,\{z-h)/\sigma_z\}^2\}\quad . \tag{5}$$

Here R is an effective reflection coefficient from the surface: if the tracer is absorbed, R = 0, while if it is perfectly reflected, R = 1. Note that the gaussian model of Eq. (5) applies to a time-average rather than to an instantaneous situation (see Fig. 3).

The parameters σ_y and σ_z are functions of down-wind distance x in the atmospheric surface layer (i.e., below about 100 m injection altitude) and of atmospheric stability classes. For near-surface injections it is customary to use the Pasquill-Gifford stability classes, which are defined in Table 3; the functions σ_y (x) and σ_z (x) from Eq. (5) are shown in Fig. 4 as a function of down-wind distance x. For tracer injection at higher altitudes it is considered better (Panofsky and Dutton, 1984, p. 245) to use the results of Brookhaven National Laboratory (BNL) experiments for injection height h > 100 m, which are also shown in Fig. 4.

Here we superpose the BNL results on the conventional Pasquill-Gifford/Turner (PG/T) curves to point out to the user that the PG/T results should not be used uncritically.

Another way to represent the dispersion diagram is to plot the horizontal dispersion distance σ_y as a function of travel time t rather than as a function of downwind distance from the source. This has the advantage that one can follow an air parcel and parameterize the spreading in terms of an eddy diffusivity coefficient K, defined by

$$\sigma_y^2 = 4\,K\,t\quad . \tag{6}$$

a. Instantaneous (from 1/50-sec exposure photograph)

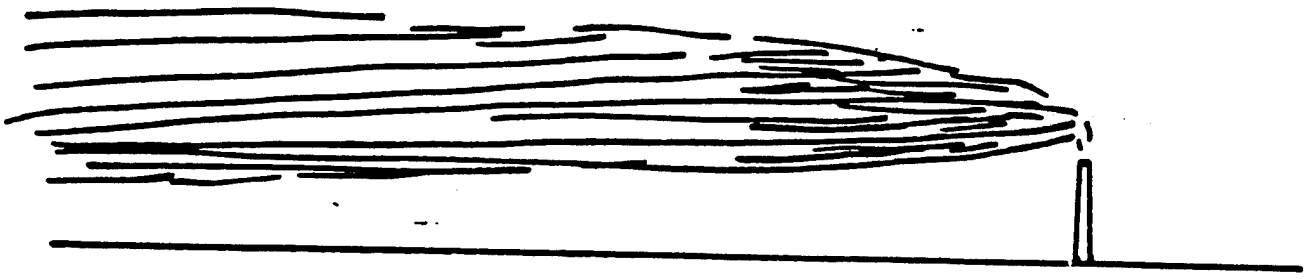

b. Average (from 5-min time exposure of the same plume)

Figure 3. The Spreading of a Stack Plume
(after Culkowski, 1961)

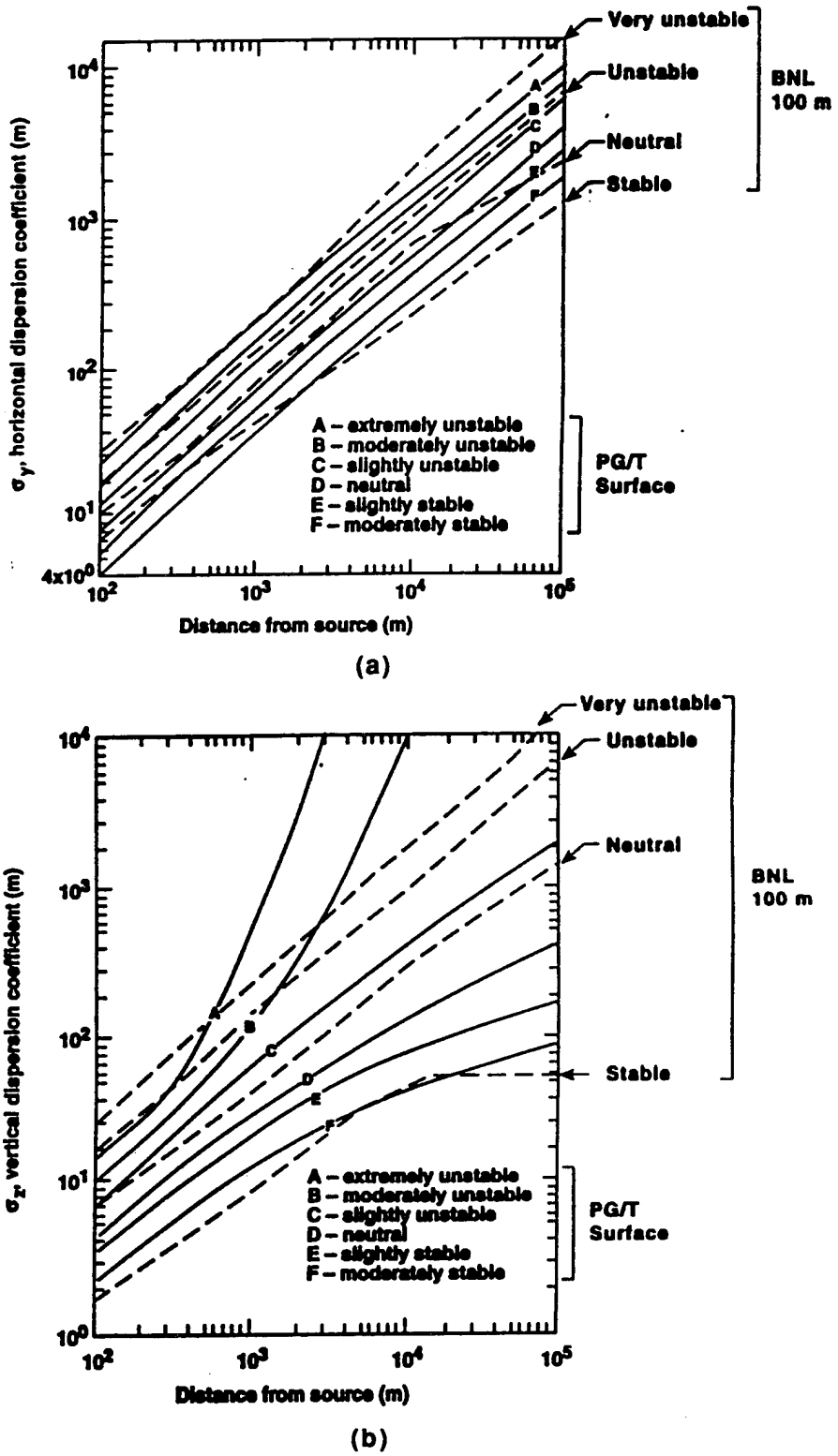

Figure 4. Dispersion Diagram for ABL Tracer Injection. We show both the Pasquill-Gifford/Turner (PG/T) near-surface model (solid lines) and the Brookhaven National Lab (BNL) results (dashed lines) for injection at altitude.

Figure 5 shows a dispersion diagram from Bauer, 1983, giving the Hage, 1964, mean (line II) and bounds (lines I and III), and also Bauer's revised upper bound (line IV). Note from the figure that:

1. The time scales of Hobbs and Ramage correlate quite well with the "new" bounds of lines I and IV, but not with the "old" bounds of lines I and III. Data from the Kuwait oil fires of 1991 as well as other recent observations fit well with the bounds of lines I and IV.[9]
2. Figures 4 and 5 are generally consistent for reasonable values u ~ 2–10 m/sec (4–20 mph) and representative ranges of Pasquill-Gifford stability parameters of Table 3.
3. The effective eddy diffusivity coefficient K increases with increasing scale of motions. Very crudely,

$$K \sim \sigma_y{}^a \varepsilon^b \quad , \tag{7}$$

where ε is the turbulent dissipation rate of the atmosphere (watt/kg, or m^2/sec^3). Some representative numerical values for ε are the following:

10^{-4}–10^{-3}	w/kg	in the lower atmosphere (0–30 km altitude)
0.1–1	w/kg	in the upper atmosphere (80–110 km altitude)

(see, e.g., Bauer, 1983, Table 3, where the sources are cited). Numerical values for the parameters a and b are, respectively (1.2 ± 0.1) and (0.2 – 0.8), for scale of 10 meters $< \sigma_y <$ 100 km.

2.4 STRUCTURE OF THE ABL OVER LAND

The ABL over land is characterized by a strong diurnal variation in temperature and (in magnitude and direction of) heat transfer, and also by relatively strong wind shears. What happens is that the sun heats the land surface in the daytime by some 10–15 °C, and radiative and convective heating from the surface produce diurnal heating (and nocturnal cooling) of the ABL. Regarding wind, along the (land or water) surface there is essentially zero wind, while above the ABL the wind has roughly the geostrophic value v_g of Eq. (2).

Figure 6 sketches the diurnal variation of temperature in the ABL over land, indicating the complex interaction of solar heating, convection, radiative cooling, and

---

9 Frank Gifford, private communication.

different levels of stability. (In the case of cloudy and windy conditions of neutral stability, this diurnal variation is suppressed.)

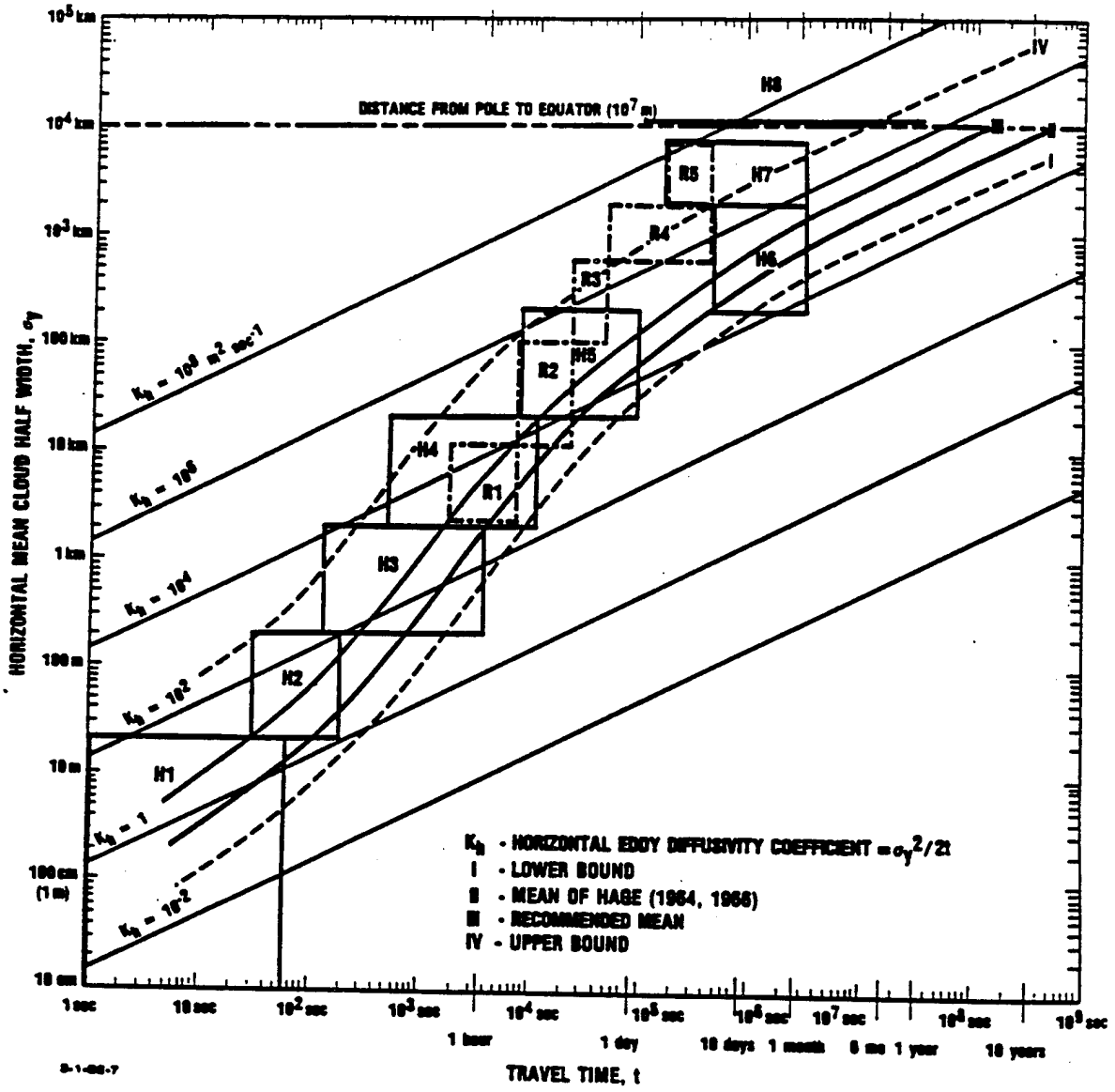

Figure 5. Dispersion diagram from Bauer, 1983, showing the Hage, 1964, Mean (Line II) and Bounds (Lines I and III), and also Bauer's revised Upper Bound (Line IV). The blocks H1–H8 and R1–R5 indicate space-time scales of atmospheric motions from Hobbs, 1981, and Ramage, 1976, specified in Table 1 above.

a. Night & early morning, before sunrise
The ground is cooler than the air, mainly because it is a more efficient thermal radiator.

b. Late morning, after sunshine has heated the ground (which absorbs sunlight much more efficiently than does the air, i.e. is warmed by radiation.) The air is then heated from the warm ground by turbulent convection, inducing thermals which enhance turbulence, heat the ABL and raise its temperature, producing unstable stratification as a result of the buoyancy-induced turbulence.

c. Late afternoon-nightfall. The air is warmer than the ground, largely because in the net cooling the ground radiates more efficiently than does the air, and thus stable stratification is re-established.

* There may be an inversion at the top of the ASL as a result of heat flux from air to ground

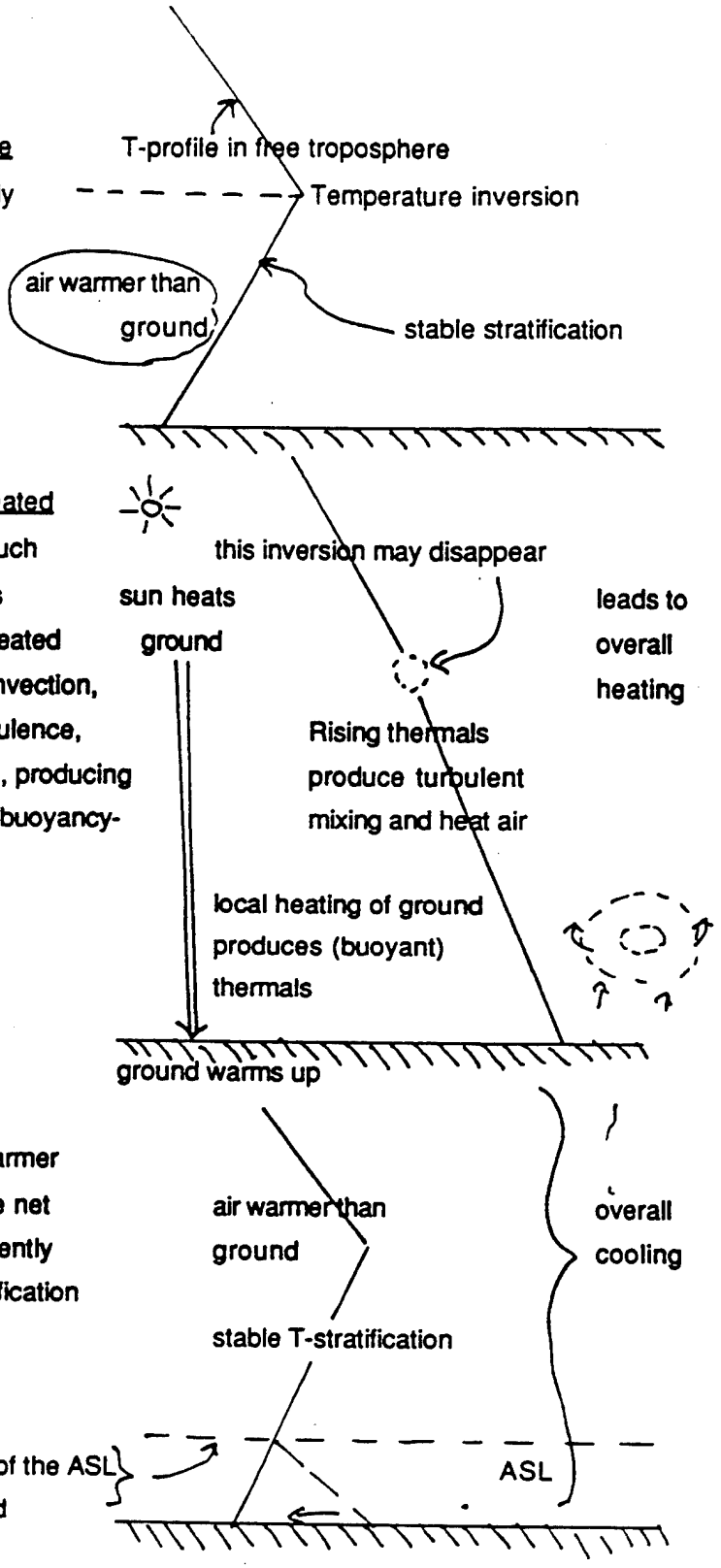

Figure 6. Diurnal Change in Temperature Profile in ABL over Land

The ABL is largely turbulent, principally as a result of wind shear, which is endemic near the surface unless it is absolutely calm. In this case the atmospheric turbulence is characterized by the Richardson's number instability Ri, where Ri is a dimensionless parameter related to the vertical gradient of the potential temperature θ and of the horizontal component, u, of the wind velocity

$$\mathrm{Ri} = (g/\theta)\, \partial\theta/\partial z \,/\, (\partial u/\partial z)^2 \quad . \tag{8}$$

In general, a region is turbulent if $\mathrm{Ri} < 0.25$.

In the ABL there is frequently also thermal convection which itself drives turbulence, since normally the motion is too vigorous for molecular viscosity to maintain laminar flow. The dimensionless parameter characterizing this turbulence is the Rayleigh number Ra,

$$\mathrm{Ra} = (g\, \Delta\theta)\, h^3/(k\nu\theta) \quad , \tag{9}$$

where $\Delta\theta$ is the lapse in potential temperature in a layer of (vertical) thickness h; here k is the thermal conductivity and ν is the kinematic viscosity.[10]

The boundary layer is largely driven by the diurnal variation in solar heating of the land surface, and this accounts for the strong thermal turbulence which generally occurs in this region. Figure 7 indicates how the temperature profile of the ABL over land may evolve with the diurnal cycle for the specific example of fall in Oak Ridge, Tennessee. At 6 a.m. with the surface temperature near its minimum value, the temperature increases up to perhaps 200 m and then stays constant up to ca. 800 m where it reaches the "standard" atmospheric temperature profile, which corresponds to a falloff of temperature with height at the dry adiabatic lapse rate, $\gamma_d = 9.8$ °C/km or θ = constant [see Appendix A, below, Eq. (A.6a)]. As the sun warms the surface, the surface temperature rises with an intermediate minimum just above the ground (8 a.m.); by 10 a.m. the minimum has disappeared as the near-surface air warms up, and by 12 noon the temperature approaches the "standard" profile, which is attained around 4 p.m. At 6 p.m., as the ground cools, so does the near-surface temperature; by 12 midnight the surface temperature is approaching its minimum value, and so is the profile below ca. 600 m. In the absence of clouds, the ABL is stable during the night and unstable in the daytime.

---

[10] For a discussion, see, e.g., McIlveen, 1992, p. 303 ff.

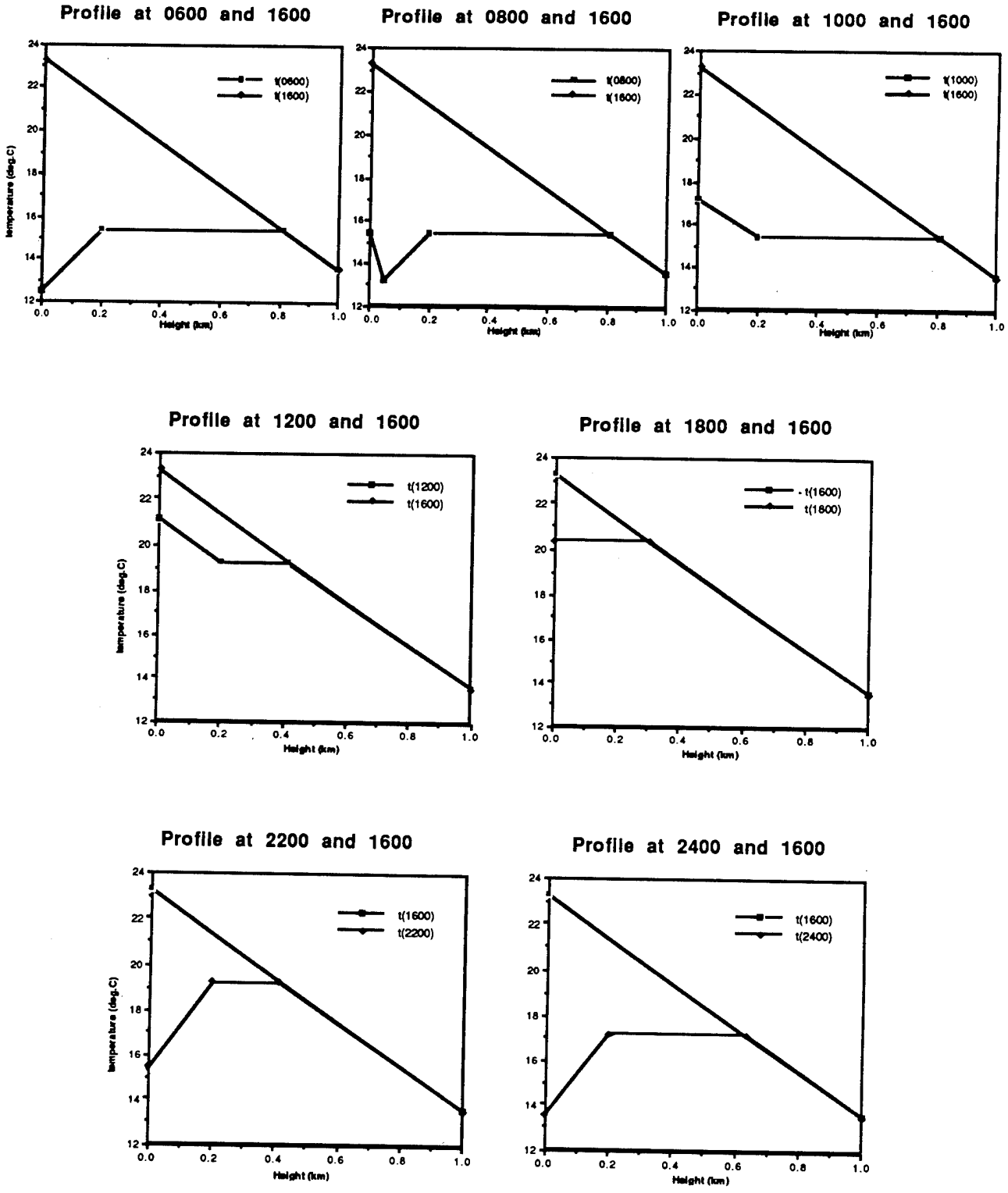

Figure 7. Diurnal Variation in the ABL: A Representative Profile over Land (Source: Slade, 1968)

It is possible to divide the ABL into several domains which vary with the diurnal cycle; note that the following division is not universally accepted.

- Laminar sublayer. Immediately next to the surface, in the lowest cm or so, there is a laminar sublayer, a region not frequently discussed in a meteorological context, although it is very important for the biophysics of plants. Note that the latent heat of atmospheric water vapor is a very important carrier of atmospheric energy, and vapor transport through the laminar sub-layer is several orders of magnitude greater than vapor transport through the troposphere as a whole (see, e.g., Section 2.7).
- "Unstable" or "Superadiabatic" Sublayer (USL). Geiger, 1965, has pointed out that over land in the presence of solar illumination (for solar elevation angles greater than ~ 10°) there is an unstable sublayer (USL), whose maximum height is of order 30–40 m at noon in June, or 4 m at noon in December. Figure 8 gives the temperature gradient and temperature profile in this region as a function of height, for both June and December. This figure is discussed in some detail in the following Section 2.5.
- Atmospheric Surface Layer (ASL). The lowest 50–200 m, say 10 percent of the ABL, is a very important region for us, because that is where humanity and the rest of the biosphere live and where most industrial effluents are deposited. This region is discussed in Section 2.5 below.
- Stable (Nocturnal) Boundary Layer (SBL). At night there is generally little wind in the ABL, and this region grows during the night.
- Convective (Mixed) Layer (ML). As the sun rises and induces convection, this region becomes well mixed.
- Residual Layer (RL). That portion of the previous day's ABL that does not get caught up in the (nocturnal) SBL.
- Cloud Layer (CL). The top of the RL, just below the capping inversion, where clouds form as a result of moisture transported upward by atmospheric convection.
- Free Atmosphere (FA). The region above the ABL where little interaction with the ground—and so little diurnal variation—takes place.

Figure 9 shows how these various regions evolve together during a 24-hour cycle.

The day/night variation is most striking over a desert or other dry land environment, as the relatively low heat capacity of a dry medium leads to large day/night temperature differences; over moist terrain it is smaller and over the ocean it is particularly small. Typical values are 10–15 °C for mid-latitude terrestrial systems as against 0.1 °C for the

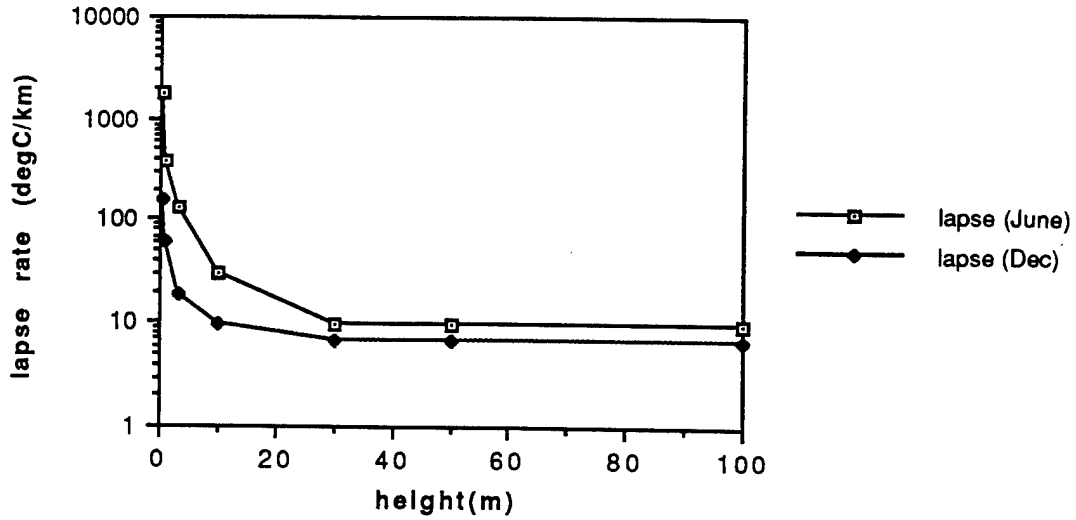

a. Temperature Lapse Rate

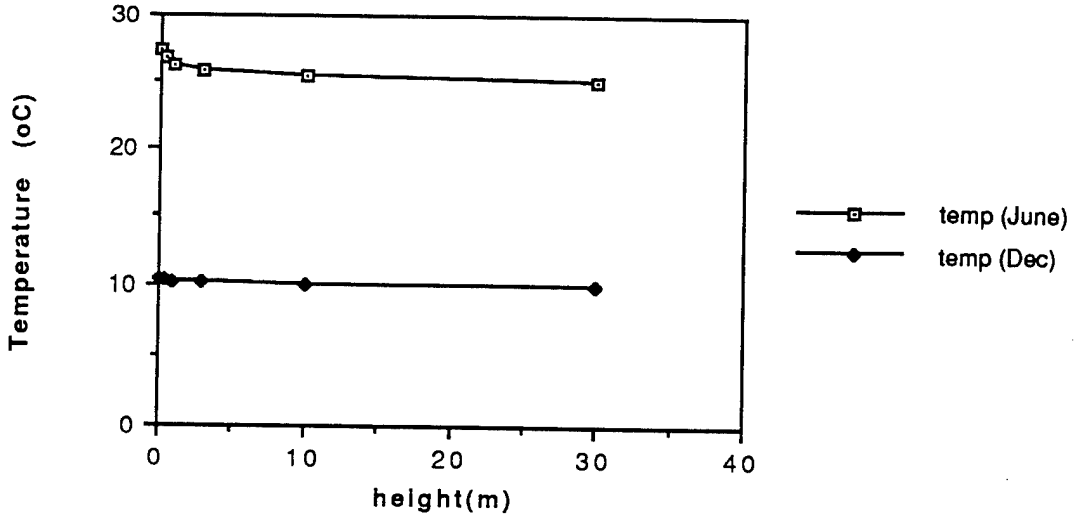

b. Temperature Profile

Figure 8. Temperature Lapse Rate and Temperature Profile over Land, at Noon in June and December. (Source: Geiger, 1965)

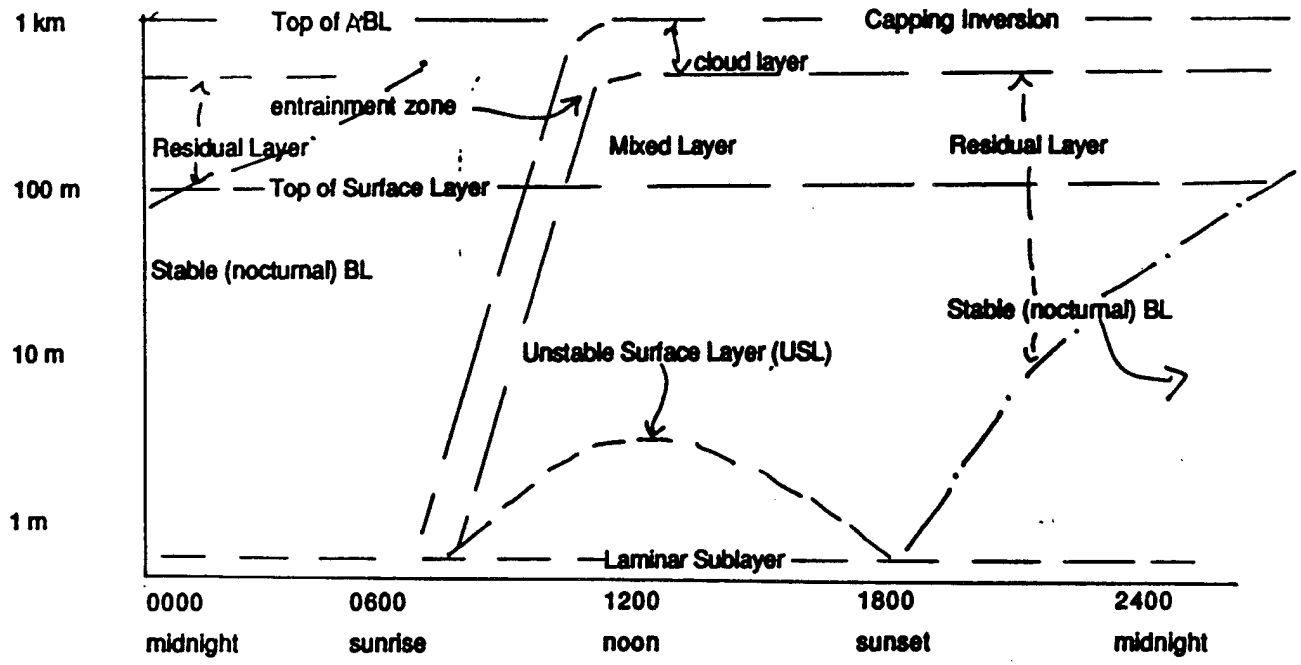

Figure 9. Diurnal Evolution of Different Parts of the ABL Schematic

ocean at mid-latitudes. Representative values of diurnal as well as annual temperature differences at the surface of the Earth are indicated in Table 4.

One important physical effect to be noted is the relatively frequent occurrence of clouds in the temperature inversion at the top of the ABL—in the *Cloud Layer* (CL). This occurs because warm moist air cools on rising (the adiabatic rise of an air parcel) and so its excess moisture condenses out. This is particularly likely to occur near the inversion at the top of the ABL above which increased atmospheric stability inhibits further cloud rise. Figure 10 shows the strong variation of water saturation vapor pressure with temperature. The effect of atmospheric moisture on the energetics of the atmosphere is extremely important, because while the atmosphere as a whole has a water vapor mixing ratio of order 10^{-2} or less, during normal diurnal temperature changes of order 10–15 °C about the mean the effective heat capacity of atmospheric moisture (largely as latent heat of evaporation and condensation) is comparable to the effective heat capacity of all the rest of the (dry) atmosphere.

Table 4. Environmental Temperature Variability Under Different Conditions

A. Diurnal Variability.

Mid-latitude ocean	(shipboard)	0.4 °C	Roll, 1965, p. 368
Mid-latitude terrestrial:			
Washington, DC (humid continental)		10 °C	"Normal weather records"
Central Germany (Giessen) - swamp, swamp land and granite rock		10 °C	Valley, 1965, Table 3-17 p. 3–21
Central Germany, sandy heath		17 °C	
Medicine Hat, Alberta, Canada (50°N. 111°W)			Barry and Chorley, 1976, p. 235
	summer	15 °C	
	winter	10 °C	

See also Geiger, 1965

B. Annual Variability (Source: *Encyc. Britannica*, 1973 Ed., Vol. 5, p. 920, Fig. 8)

Tropical ocean, rain forest	3 °C
Mid-latitude ocean	5–10 °C
Mid-latitude continental	20–30 °C
Desert (Sahara)	25 °C
Polar regions: Alaska, Yukon, Siberia, Antarctica	to 50 °C

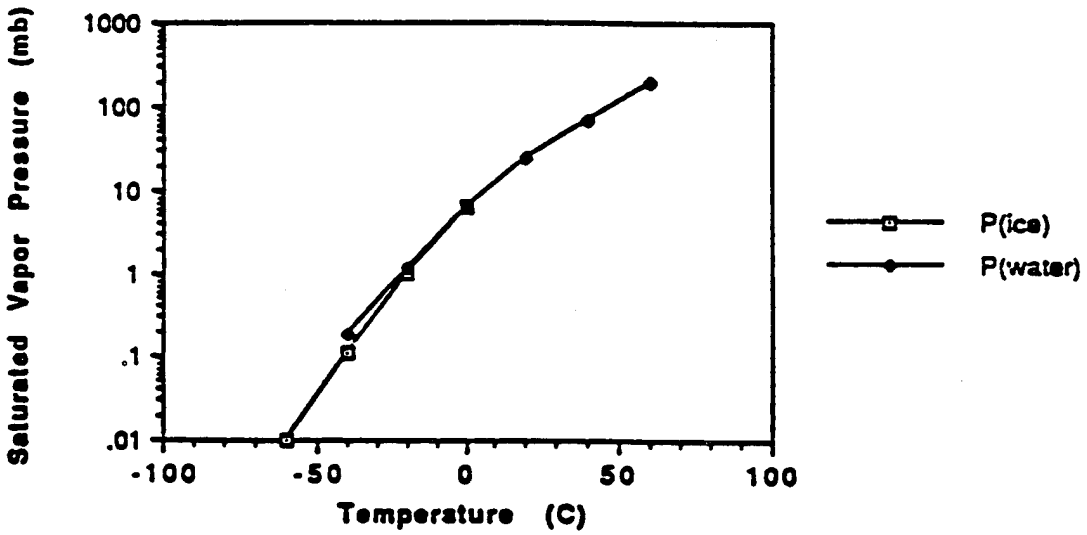

Temperature (°C)	Water Vapor Mixing Ratio (g/kg air)
−10	0.0018
0	3.3
10	6.6
20	12.5
30	26.1
40	45.3

Figure 10. Saturation Vapor Pressure of Water and Over Ice as Function of Temperature (Source: List, 1984, p. 351 ff.)

Another aspect of the dynamics driven by solar heating and the consequent diurnal temperature variation that is shown in Figs. 7 and 9 has to do with atmospheric turbulence, which reflects the atmospheric response to wind shears and thermal gradients. Approximately half the atmosphere's loss of kinetic energy occurs in the ABL, and much of the rest is associated with clear air turbulence (CAT) near the tropopause (see, e.g., Panofsky and Dutton, 1984, and McIlveen, 1992, esp. p. 301 ff.). Indeed, the ABL is the region of the atmosphere in the most constant and vigorous turbulent motion.

2.5 THE ATMOSPHERIC SURFACE LAYER (ASL) OVER LAND

While most of the interaction between the atmosphere and the underlying Earth and ocean occurs in the ABL (which represents about 10 percent of the mass of the atmosphere), the most dramatic effects take place in the atmospheric surface layer (ASL), or roughly the lowest 10 percent of the ABL. As human beings, we are of course most interested in the ASL because this is where we live and also where most of our industrial effluents are deposited. It is here that the effects of surface roughness are important. Evidently the (horizontal) wind is zero along the surface, and it rises to its free-atmosphere (geostrophic) value at a rate depending on the geometric scale of the surface features and there is both the largest diurnal variability as well as variability with the atmospheric stability parameters.

Figure 11 shows the wind profile in the lowest portion of the ABL as a function of surface roughness and also of atmospheric stability. Table 5 shows representative values of the surface roughness length parameter z_o and of the roughness height h_s which is approximately equal to the thickness of the surface layer.

Empirically, one may express the wind speed u(z) at height z as

$$v(z) = (u^*/k) \ln[(z-d)/z_o] \quad , \tag{10}$$

where $d \sim (2/3)\, h_s$ is the (empirical) zero-plane displacement.

The wind profile in the surface layer is discussed in more detail in Sections 3.2–3.4.

Figure 8 shows the temperature falloff ("lapse rate") and temperature profiles over land at noon, based on a detailed survey of observations in the lowest 100 m of the atmosphere in Europe and Egypt (Geiger, 1965, p. 77 ff.). In June the lapse rate above about 30 m is equal to the dry adiabatic lapse rate, DALR = γ_d = 9.8 °C/km, while in

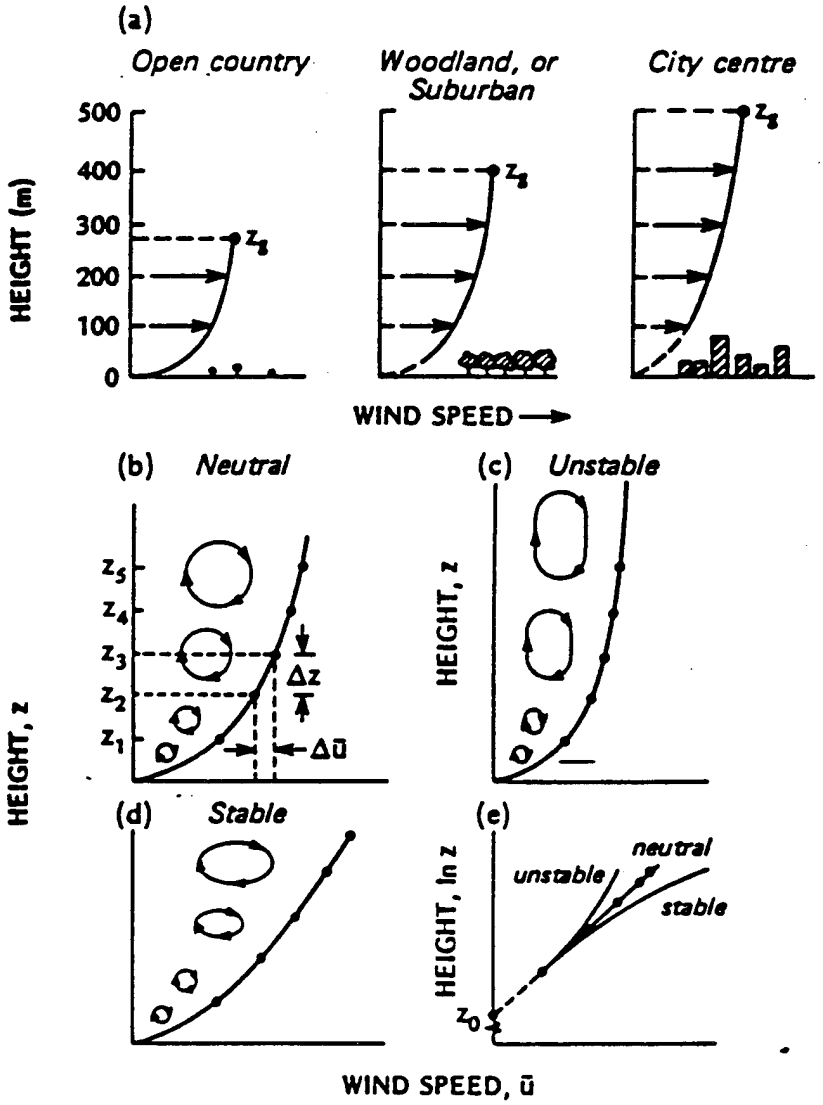

The wind speed profile near the ground including: (a) the effect of terrain roughness (after Davenport, 1965), and (b) to (e) the effect of stability on the profile shape and eddy structure (after Thom, 1975). In (e) the profiles of (b) to (d) are plotted with a natural logarithm height scale.

Figure 11. Wind Profile near the Ground as Function of Surface Roughness and Atmospheric Stability. (Source: Oke, 1978, p. 45)

Table 5. Roughness Scales for Different Surfaces (Source: Monin, 1970; Oke, 1978)

Surface	Remarks	z_o, roughness length (m)	$h_s \sim v/u_*$ roughness height[a]
Water[b]	still to open sea	$0.1–10 \times 10^{-5}$ [c]	
Ice	smooth	10^{-5}	
Snow		$0.5–10 \times 10^{-4}$	
Sand, desert		3×10^{-4}	
Soils		$10^{-3}–10^{-2}$	
Grass	mowed	$2–7 \times 10^{-3}$	1.5–3 cm
	high	0.9(?9?)–3.7	60–70 cm for wind speed 1.5–6 m/sec (larger speed causes stems to bend)
	0.02–0.1 m	$3 \times 10^{-3}–10^{-2}$	d < 0.07 m[c]
	0.25–1 m	0.04–0.10	d < 0.66 m
Agricultural crops		0.04–0.2	d < 3 m
Shrubs		0.1	
Orchards		0.5–1.0	d < 4 m
Forests:	Deciduous	1–6	d < 20
	Coniferous	1–6	d < 30
	From Monin, 1970	0.5–1	10 m
Cities		1	

---

[a] From Monin, 1970.

[b] z_o depends on wind speed.

[c] From Oke, 1978, p. 48, there is also a zero-plane displacement d, and $v_1(z) = (u_*/k) \ln [(z-d)/z_o]$. Here d is taken as (2/3 h).

December the lapse rate above 30 m is approximately 6.6 °C/km. This smaller lapse rate reflects on high cloudiness in winter (cf. McIlveen, 1992, p. 123). Closer to the surface, the lapse rate at midday (under the influence of solar irradiation) increases very strongly, although the surface temperature increase is quite moderate.[11]

This very rapid falloff of temperature above the surface may lead to an increase in density with height[12] which may produce dramatic effects of refraction, such as (desert) mirages (see, e.g., Minnaert, 1993).

This lowest region [which I call the unstable sublayer (USL)] is formed when the solar elevation angle reaches 10° and has a maximum at local noon, with a maximum height of ~ 5 m in December or 50 m in July.[13,14] A comparable "superadiabatic layer" is also observed over the ocean (see Section 2.6, in particular Fig. 13; and Roll, 1965, pp. 264–265, 275, 305).

2.6 THE ABL OVER THE OCEAN

As has been pointed out, due to the large heat capacity of the ocean, the day-night temperature difference over water is very small compared with that over land. However, the air (near-surface) temperature may differ significantly from the water surface temperature, and the air-sea temperature difference (ASTD).[15]

$$\mathrm{ASTD} = \mathrm{T(air)} - \mathrm{T(sea)} \qquad (11)$$

is a useful parameter for determining the temperature profile in the marine ASL and ABL.

One may ask how ASTD values are obtained. From about World War II until the 1970's there were a number of weather ships on the oceans, mainly in the North Atlantic, and they measured T(air) at deck or mast level and T(sea) either by scooping a bucket of

---

11 Anybody who goes to the beach on a sunny day must be familiar with the fact that the ground may be "burning hot" while the air is just pleasantly warm.

12 When the rate of falloff of T with height exceeds 34.2 °C/km, the atmospheric density actually increases with height (see Geiger, 1965, pp. 85 and 135).

13 The relation of the USL to the Atmospheric Surface Layer (ASL) may not have been established.

14 As far as I know the data only apply to midlatitudes in Europe and Egypt, i.e., there could well be some latitude variation. Note that the standard anemometer height is 10 m over a smooth surface, while temperature and humidity are typically measured in an enclosure at height of 1–1.5 m. Thus from the nature of measurements it is possible that the USL is frequently overlooked.

15 cf. Dion and Leclerc, 1990, and Trahan, 1995. Note that ASTD is measured over a 10–20 m vertical interval, while typically stability refers to the Atmospheric Surface Layer, which is typically 100–150 m thick—but see footnote 6 in Section 2.3 above.

water from the sea and measuring its temperature or else by reading the temperature of the sea water that enters the condenser intake of the ship.[16]

There is a limited amount of work on atmospheric stability over the oceans, based largely on observations taken from weather ships:

- The weather ships provided much more information than previous weather reports over the oceans, which were provided by merchant ships that just happened to be passing through a given location.
- By now we get a great deal of data from weather satellites, but of course this gives much less detail of near-surface effects than did the weather ships.
- For some examples on maritime air masses, see Dion and Leclerc, 1990. Note that the day-night difference in stability conditions over water is unlikely to be large, but the influence of air masses, frontal passages, and storm tracks will be important.[17]
- In general, at mid- to high latitudes the atmosphere over the eastern side of the oceans is stable with low-level inversions; note the stable layer of stratus clouds off the California coast.
- By contrast, air over the western side of the oceans is very unstable in winter, with cold air masses coming off the continents of Asia and America and producing a deep, unstable mixed layer.
- Over the broad ocean between the continents there is a transitional zone.
- In the North Pacific there are lots of storms with mechanical mixing, with strong mixing on both sides of the storm track.
- The character of the air masses will vary strongly near the continent-ocean boundaries; this variability will be less critical in the open ocean, except in the storm tracks of extra-tropical cyclones.
- A great deal of data from the weather ships is available—e.g., at NOAA—but has apparently not been analyzed.

---

16 Some 2 m below the surface. Cf Roll, 1965, Ch.2; p. 15 in Roll shows the locations of the oceanic weather ships.

17 When warm air passes over cold water, there will tend to be fog, while if cold air moves over warm water there is likely to be a cloud deck; but below this cloud deck the lapse rate is likely to be more unstable than on the average.

To summarize:

- When the atmospheric lapse rate is unstable, the high-altitude density is *large* (because T decreases with height), thus light rays are bent *down*, and thus the visual range is *reduced*[18] (relative to "normal" or *neutral* conditions).
- When the atmospheric lapse rate is *stable*, the high-altitude density is relatively *small* (because T increases), thus light rays are bent *up* and so the visual range is *increased.*
- When the atmospheric lapse rate is *neutral*, the temperature gradient lies in the range of – 6 to – 10 °K/km (the dry and saturated adiabatic lapse rate of air, respectively) and quasi-horizontal light rays in such an atmosphere are slightly curved, being concave down with a radius of curvature of about 40,000 km, as a result of the atmospheric pressure gradient due to the Earth's gravitational field.[19]

Much of the time, ASTD < 0, i.e., the sea is warmer than the air; the reverse is only found in certain, mainly coastal, regions, where upwelling occurs or cold currents dominate.[20] Table 6 indicates schematically how atmospheric stability over water is related to ASTD. Note that:

1. This describes the atmospheric conditions in lowest 40–100 m above the sea surface.
2. *Neutral conditions* correspond to the case when the air temperature falls with height at the adiabatic lapse rate (ALR) - note that this may include effects of moisture, which can make a big difference[21]. In meteorological usage, this may be termed "Lapse" (i.e., temperature falls/lapses with increasing height).
3. *Unstable conditions:* temperature falls with height more rapidly than the ALR—also described as "Lapse."
4. *Stable conditions:* described in meteorology as "Inversion," these conditions correspond to the case in which air temperature falls with temperature less rapidly than the ALR or increases with height.

---

18 This is significant mainly over the ocean with its uniform surface, because over land there tend to be hills and valleys so that the relatively small effects of refraction are obscured by larger, geometrical factors.

19 I wish to thank Prof. Lehn for clarifying this point for me.

20 Cf. Roll, 1965, p. 290. However, when a warm front passes over the ocean one clearly has ASTD > 0 locally.

21 At room temperature, the dry adiabatic lapse rate (DALR) is 9.8 °C/km, while the moist (saturated) adiabatic lapse rate is ~ 6 °C/km.

Table 6. Meteorological Stability Over Water as Function of ASTD (Air-Sea Temperature Difference) (Source: Trahan, 1995)

Conditions	Unstable	Neutral	Stable
Temperature Gradient	Lapse - $\partial\theta/\partial z < 0$	Lapse - $\partial\theta/\partial z = 0$	Inversion - $\partial\theta/\partial z > 0$
ASTD (= T(air) – T(sea)	< 0	0	> 0
Weather	Sunny, daytime	Cloudy, windy, day or night	Night, clear, calm

5. Models work best under lapse conditions. Under inversion conditions the stratified temperature profile cannot be determined by just two temperature measurements. In fact, the most interesting situation is a thermocline, or temperature inversion, when most of the temperature rise occurs within a narrow range of altitudes.[22]

6. The relative frequency of occurrence of neutral, unstable, and stable conditions depends on location and on cloud cover

Figure 12 shows some "representative" profiles that indicate in qualitative terms how changing the sign of ASTD changes the overall character of the temperature profile.

1. The numerical values of Fig. 12 come from some computations performed by Arete Associates.[23] They correspond to a midlatitude summer atmosphere with a wind speed of 4.3 m/s at 10 m altitude. The Arete profiles extend only up to 40 m but have been extended here in schematic form up to several hundred meters.

2. Near the surface the temperature changes quite rapidly to approach the "normal" profile for ASTD = 0, which simply demonstrates a falloff of temperature with height at the adiabatic lapse rate.[24] This would presumably continue up to the tropopause, which generally lies at approximately 11 km at mid-latitudes.

3. When ASTD > 0 (i.e., we have warm air over cold water), above a few meters in height (~ 5 m for the case of Fig. 12) the temperature falls off with height at the adiabatic lapse rate.

---

22 The term "thermocline" is normally used in the context of under-surface water temperatures; Liljequist apparently first applied this term to atmospheric (rather than oceanic) temperature gradients.

23 IRTool Algorithm Description Document, August 1994; Atmosphere Section, Fig. 1, p. 19.

24 For unsaturated air, one assumes a falloff at the dry adiabatic lapse rate of 9.8 °C/km, rather than at the saturated adiabatic lapse rate ~ 6 °C/km.

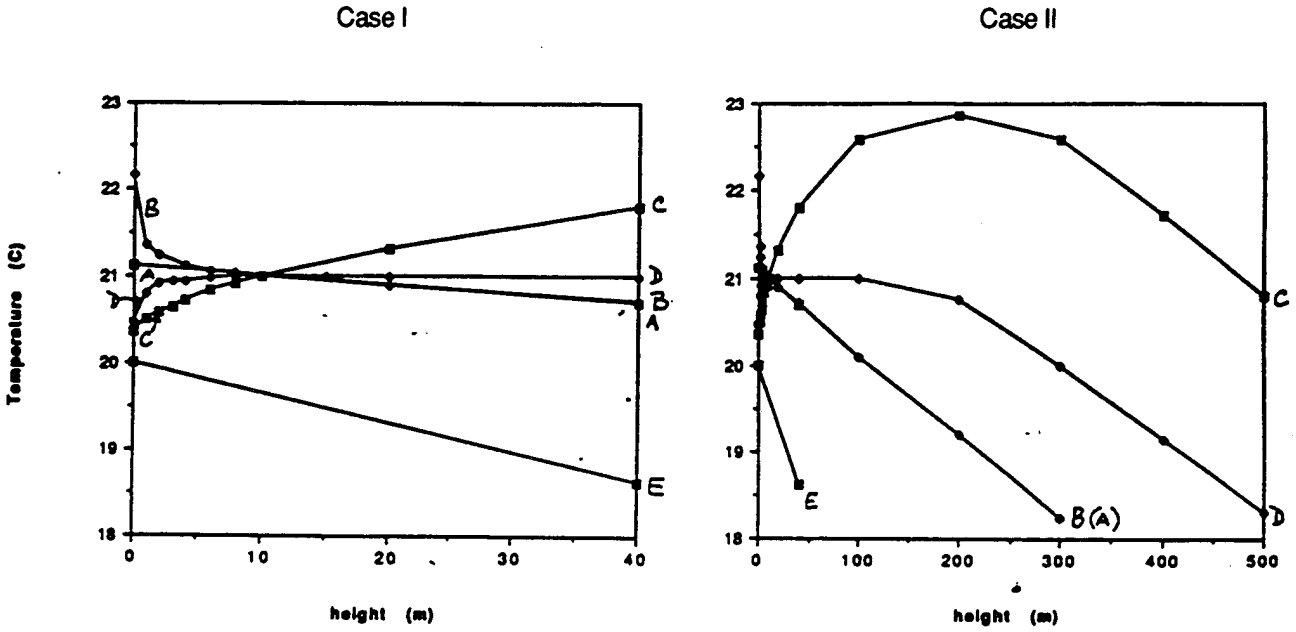

Note the presence of an inversion (temperature increasing with height) when ASTD > 0, but at sufficiently high altitudes (100–1,000 m) the temperature reverts to a normal (lapse) rate. Figure 12 Case I (heights < 40 m) come from Arete computations, while Fig. 12 Case II (heights up to 500 m) have been extended and are only qualitatively significant.

Curves:

- A: ASTD = 0 - uniform lapse
- B: ASTD < 0 - rapid falloff near (warm) sea surface, then uniform lapse
- C: ASTD > 0 - rapid increase near (cold) sea surface, maximum at high altitudes (100–1,000 m), then goes to uniform lapse
- D: ASTD > 0 but twice the wind velocity (8.6 m/s vs. 4.3 m/s). The strong wind forces conditions closer to neutral at high altitudes (i.e., much smaller maximum*).
- E: Lapse rate 34.2 °C/km - if the temperature falls off more rapidly than this, the air density increases with height.

* With u_0 = 8.6 m/s, the curves for ASTD ≤ 0 hardly differ from those at u_0 = 4.3 m/s.

Figure 12. Schematic Temperature Profile in ABL Over Ocean as Function of Air-Sea Temperature Difference (ASTD)

4. When ASTD < 0, so that we have cold air over warm water, the behavior is different. There is an *inversion* [i.e., the temperature increases with height (very rapidly up to perhaps 5–10 m, and then perhaps 3–4 times as fast as the decrease corresponding to the adiabatic lapse rate)]. Clearly this does not go on "for ever," but must turn around above some altitude of perhaps 100–1,000 m, above which it falls off with height at the "standard" adiabatic lapse rate.

5. Arete also made calculations at 8.6 m/s, twice the wind speed cited above. There is little change for ASTD < 0, but when ASTD > 0 there is only a very minor inversion with a very slight and broad temperature maximum, which is shown schematically in Fig. 12 Case I. This different behavior is understandable, since a high wind induces higher levels of turbulence that wash out many of the detailed features in the profile, such as replacing the various atmospheric stability classes of Table 3 by the simple case of neutral or "D" stability. At altitudes above the maximum the temperature will fall off with the normal (adiabatic) lapse rate.

6. Note that because the sea surface temperature shows negligible diurnal variation, the present temperature profiles apply to all times of day, unlike the case of temperature profiles over land that are shown in Fig. 7.

Other elements of phenomenology are shown in Fig. 13, which gives a schematic vertical cross section of the trade wind moist layer over the Caribbean Sea. We see the altitude range in which cumulus clouds lie, and also representative profiles of the potential temperature, θ, and of the water vapor mixing ratio κ for this situation.

- θ remains constant throughout the mixed layer, which corresponds to neutral (D) stability.
- The water vapor mixing ratio κ stays constant throughout the mixed region, which makes sense physically, but it falls off significantly at higher altitudes as we get away from the ocean.
- In Fig. 13 we also show a superadiabatic layer near the surface. Typically the height of this is 0.03 times the height of the mixed layer under lapse conditions. This is where the large temperature gradient is shown in Fig. 12, e.g., Case II.

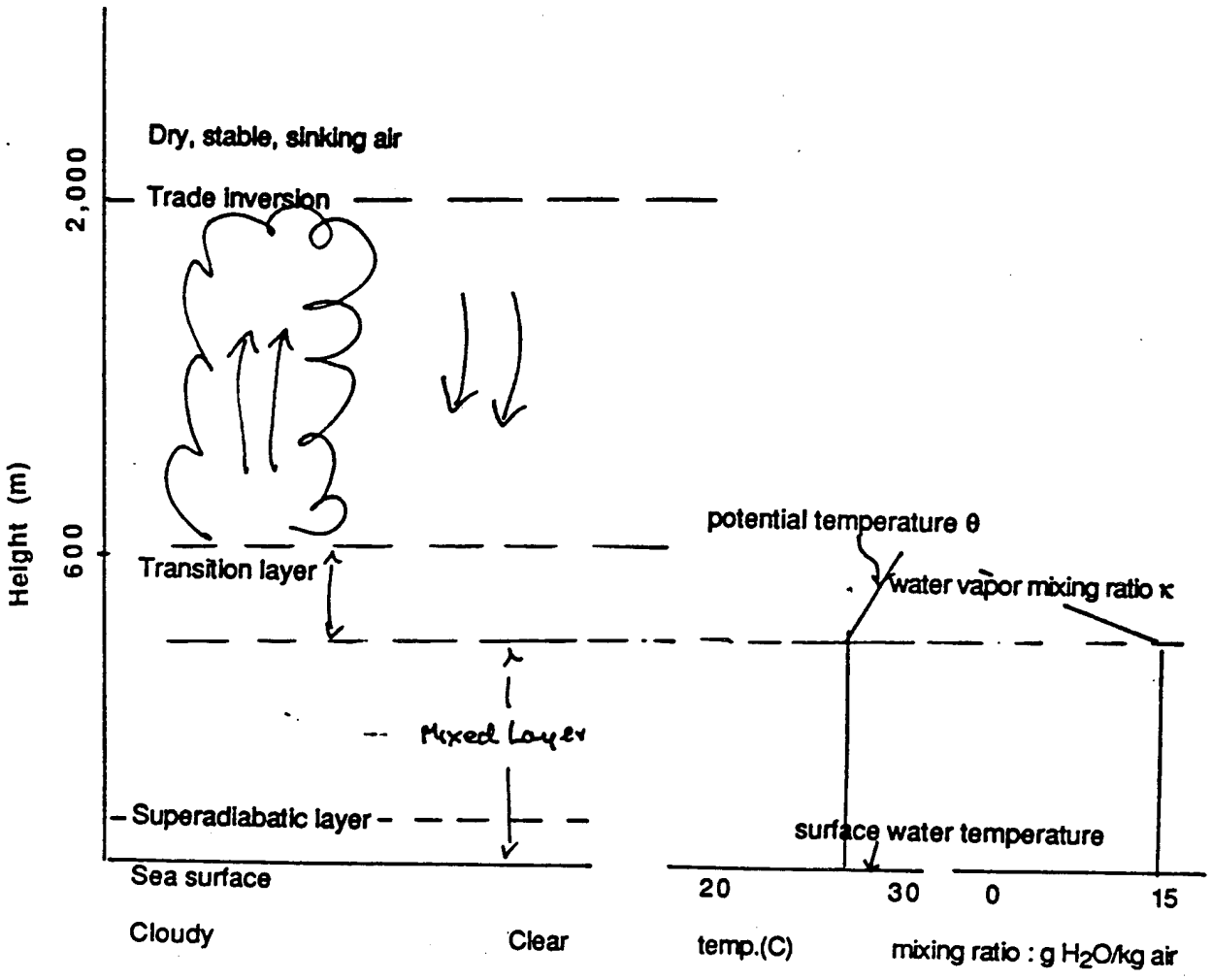

Figure 13. Trade Wind Moist Layer Over the Caribbean Sea. We show a number of different regions of the ABL over the ocean and sketch how the potential temperature θ and the water vapor mixing ratio κ may change above the mixed layer. (After Roll, 1965, pp. 292, 305)

2.7 INTERACTION BETWEEN THE ATMOSPHERE AND THE UNDERLYING EARTH OR OCEAN SURFACE

As far as the atmosphere is concerned, the Earth or ocean is not just a constant, uniform, non-interacting surface, but rather a physical medium that interchanges energy, moisture, and minor constituents with the atmosphere; its temperature changes tend to be smaller than those of the atmosphere because its density is larger than that of the atmosphere by a factor ~ 10^3.

It is appropriate to present some numbers. Munn, 1966, p. 92, quotes an estimate that 2–3 kg H_2O move across the water-air interface of thickness several mean free paths per m^2 per second; this corresponds to an energy flux of 3–5 $\times$ 10^5 W/m^2 if we associate a latent heat of 600 kCal/kg with the mass transport of water. This is to be compared with global energy flow in the Earth-atmosphere system of 600 W/m^2, so that net ground-to-air energy transfer is ~ 10^{-3} times that which goes on within a few mean free paths of the surface.

A land surface, especially one having relatively low water content and thus a relatively low heat capacity, shows large temperature changes in the top few cm, but this change damps out rapidly with increasing depth in the ground. From the figures of Geiger, 1965, Ch. II, one may see that in sandy soil the mean diurnal fluctuation is less than 1 °C at depths below 50–60 cm, with perhaps 5 percent of the fluctuation in the top 1–2 cm. However, if one looks at longer term records, one sees that at depths of order 1 meter there may still be a significant annual temperature variation (10–15 °C), comparable with the annual temperature fluctuation measured in the bottom 1–10 meters of the atmosphere (see, e.g., Table 7).

If one asks for the overall interaction between the lower atmosphere and the terrestrial land or ocean surface, the following remarks may be made:

1. Land-atmosphere and ocean-atmosphere interactions differ drastically in the small as far as temperature fluctuations go, though not obviously as far as energy transfer is concerned.

2. The above discussion of surface temperature fluctuations as a function of depth and time scale can clearly also be applied to the ocean, at least in a qualitative sense (see Table 7). Evidently, the longer the time scale under consideration, the more mass of solid or liquid "earth" interacts with the atmosphere, and thus the greater is the effective inertia of the Earth-atmosphere system which

Table 7. Characteristic Time Scales in Atmosphere and Surface

Process	Time Scale[a]	Source
Energy exchange in the troposphere	1 week	Tennekes, 1974, p. 59[b]
Reaction to turbulent heat and moisture fluxes	3 days	"
Viscous dissipation of kinetic energy	1 day	"
Latent heat dissipation	1 day	"
Reaction to radiative fluxes	1 week	"
Characteristic atmospheric residence time of inert tracer:		
in stratosphere	1–5 years	Reiter and Bauer, 1975, see Fig. 15
in free troposphere	7–30 days	"
in ABL	1–3 days	"
in ASL (< 50–100 m)	– 6 hours	
Land-atmosphere temperature equalization:		
top 20 cm	1 day	Geiger, 1965
top 1 m	1 year	"
Ocean-atmosphere temperature equalization:		
top 1 cm	1 day	Roll, 1965
top 1 m	1 year	"

[a] All measures are highly tentative.

[b] Most of Tennekes' estimates apply to the ABL.

determines the climate. Some representative time scales are listed in Table 7, but they must be interpreted with all kinds of cautions.

3. In addressing the overall (long-term/climatic) problem of the interaction of the Earth with the incident solar radiation, the oceans are important: a significant fraction, perhaps as large as 40 percent of the meridional (pole-to-equator) energy transfer seems to be carried by ocean currents.[25] However, it may well be that the standard near-surface temperature recorded for meteorological/ climatological purposes is a useful indicator for oceanic effects also, insofar as changes in near-surface temperature induce changes in below-surface temperature and thus also in other below-surface characteristics, such as energy transfers.

4. Most of the preceding discussion applies to land surfaces, unless it explicitly mentions water surfaces. For tropical ocean surfaces, see, e.g., Fig. 13, which shows a schematic representation of the trade wind moist layer over the Caribbean Sea; for more information on this topic, see, e.g., McIlveen, 1992, p. 421; Barry and Chorley, 1976.

5. Atmospheric stability is an important factor in the variation of conditions at different times and places (see Section 2.3 and Appendix A).

6. Note that there will be a variability on smaller scales of space and time, as well as some effects due to terrain (slope and albedo!) variability. We know that mountains affect the air flow, inducing clouds, lee waves, and turbulence on a variety of scales. Differences in ground albedo also affect the airflow, and generally there will be topographic as well as geostrophic control. There must also be corresponding—if probably smaller—effects associated with wind-driven water waves.

---

[25] Cf, e.g., CIAP Mono.4, DOT-1 Version, May 1974, p. 4-16 ff.

3.0 THE WIND PROFILE IN THE ABL

3.1 OVERVIEW

The wind profile in the ABL changes on a range of space and time scales, and is important for a variety of applications. Perhaps the best way for us to appreciate the variability of the wind on a scale of hours is to consider the Beaufort scale of wind force, which gives a measure of wind speed as indicated without instruments; this is given in Table 1 in Section 2.2 (pp. 13–14). In Section 3.2 we introduce the *geostrophic wind* $\mathbf{v_g}$, which is attained at heights well above the disturbing influences of the Earth's surface. In Section 3.3 we ask how the geostrophic wind is modified by atmospheric turbulence as the surface is approached, introducing the *Ekman spiral.* Then, in Section 3.4 we present the velocity profile in the lowest 50 m above the surface, including a convenient analytic description. Finally, in Section 3.5 we discuss the near-equatorial ABL for the case when the Coriolis factor f of Table 8 becomes very small.

3.2 GEOSTROPHIC WIND

At heights well above the disturbing influence of the Earth's surface, the average air motion is determined by the balance between the pressure gradient force $(1/\rho)$ grad p and the Coriolis interaction $[\Omega \times \mathbf{v_g}]$ arising from the centrifugal force due to the rotation of the Earth. Thus, at the top of the ABL, the mean wind is roughly equal to the geostrophic wind $\mathbf{v_g}$; at the surface, the horizontal wind is essentially zero, and the transition depends on the nature of the surface (see, e.g., Fig.11). The geostrophic wind $\mathbf{v_g}$ is given by the balance between the Coriolis force and the horizontal component of the atmospheric pressure gradient,

$$\mathbf{v_g} = (1/\rho\, f)\, [\mathbf{k} \times \mathrm{grad}_H\, p] \quad . \tag{2}$$

The various quantities are introduced in Section 2.1.

Table 8 gives numerical values of the Coriolis parameter $f = 2\,\Omega \sin\phi$ as a function of latitude ϕ.

Table 8. Coriolis Factor as Function of Latitude

Latitude ϕ	0°	1°	2°	5°	10°	20°	43°	90°
f (10^{-4} /sec)	0	.0255	.0508	0.127	0.253	0.50	1.00	1.458

Note that the Coriolis factor f is very small near the equator, where the air flow is significantly different from that at mid-latitudes (see, e.g., McIlveen, 1992, pp. 195–207). Some of the consequences of this are discussed in Section 3.5.

In evaluating the geostrophic wind, it is customary to choose local cartesian coordinates with the x-axis in the E-W direction, y-axis in N-S direction, and z-axis vertical, which gives

$$- f v_{g,y} = - (1/\rho)\, \partial p/\partial x \qquad (12a)$$

$$f\, v_{g,x} = (1/\rho)\, \partial p/\partial y \quad . \qquad (12b)$$

The geostrophic wind is a useful approximation to the actual mean wind at midlatitudes at heights $z > h$, where h (~ 1 km above the local surface) defines the top of the ABL.

3.3 EKMAN SPIRAL

Now we ask how the geostrophic wind is modified by turbulent "eddy friction" as the surface is approached. A traditional—if not very satisfactory—way to do this is to describe the equation of motion which defines the velocity **v** in terms of a virtual shear stress tensor τ_{ij} to account for the effects of turbulent dissipation, and to replace Eq. (2) by

$$[\Omega \times \mathbf{v}]_i = - (1/\rho)\, \partial p/\partial x_i + (1/\rho)\, \Sigma_k\, \partial/\partial x_k\, \tau_{ki} \quad . \qquad (13)$$

Clearly this reduces to Eq. (2) in the limit of flow far away from the surface, where the shear stress tensor τ_{ij} vanishes and $v \sim v_g$. It is necessary to make some kind of ansatz for τ_{ij}, and here one may introduce an *eddy viscosity* K by the relation:

$$(1/\rho)\, \tau_{zi} = K\, \partial v_i/\partial z \;\; (i = x,y) \quad . \qquad (14)$$

Note that K is not a constant but depends on the history of the relevant air mass and also shows some scale dependence (see discussion at end of Section 2.3, in particular Fig. 5). The hypothesis of an "eddy viscosity" for turbulence is an approximation known as "first-order closure" (see, e.g., Panofsky and Dutton, 1984, Section 4.7, p. 101 ff).

With the increasing power of computers it has proved possible to apply a significantly more sophisticated approximation to the non-linear equations of motion of the atmosphere—"second order closure"—to such applications as the SCIPUFF-PC code for tracer dispersion (see Sykes, 1994).

Now, for convenience we take the x_1-axis along the isobar so that $\partial p/\partial x_1 = 0$, the pressure gradient being assumed invariant with height in the PBL, and combine the components v_1 and v_2 of velocity to form a complex vector $U = v_1 + jv_2$ where $j = (-1)^{1/2}$. The pressure gradient term $(1/\rho)\,\partial p/\partial x_2$ is replaced by $-fG$, where $G = |v_g|$, and neglecting the change of density with height, Eqs. (12) and (13) become

$$jf(U-G) - K\,\partial^2 U/\partial z^2 = 0 \qquad (15)$$

to be solved with the boundary conditions

$$U = 0 \text{ on } z = 0 \text{ (i.e., no slip at the surface)} \qquad (16a)$$

$$U \Rightarrow G \text{ as } z \Rightarrow \infty \quad . \qquad (16b)$$

The solution to this is

$$U = v_1 + jv_2 = G[1 - \exp(-z\sqrt{(f/2K)})\{\cos z\sqrt{(f/2K)} - j \sin z\sqrt{(f/2K)}\}] \quad , \qquad (17)$$

which is usually displayed as a graph of v_1 vs. v_2, the curve—parameterized in terms of z or $z\sqrt{(f/2K)}$—being an equiangular spiral with the geostrophic wind as limit point, the *Ekman spiral.*

Figure 14 shows the Ekman spiral and also v_1 and v_2 as functions of z, both for the idealized case of Eq. (17) and also for a typical situation for which K is not a constant [so that Eq. (16) does not hold]. The solution shows that inside the friction layer the wind does not blow exactly along an isobar, but is deviated along the low pressure region. The angle between the wind and the isobar has a maximum value of 45° at the surface [because $\lim_{(z \Rightarrow 0)} v_2/v_1 = 1$] and decreases with increasing height. Also one may note that the wind attains the geostrophic direction at a height

$$h_d = \pi\sqrt{(2K/f)} \quad . \qquad (18)$$

One can identify h_d with h, and, if an estimate can be made for the eddy diffusivity K, one can infer in principle how the ABL varies with latitude through the Coriolis factor f.

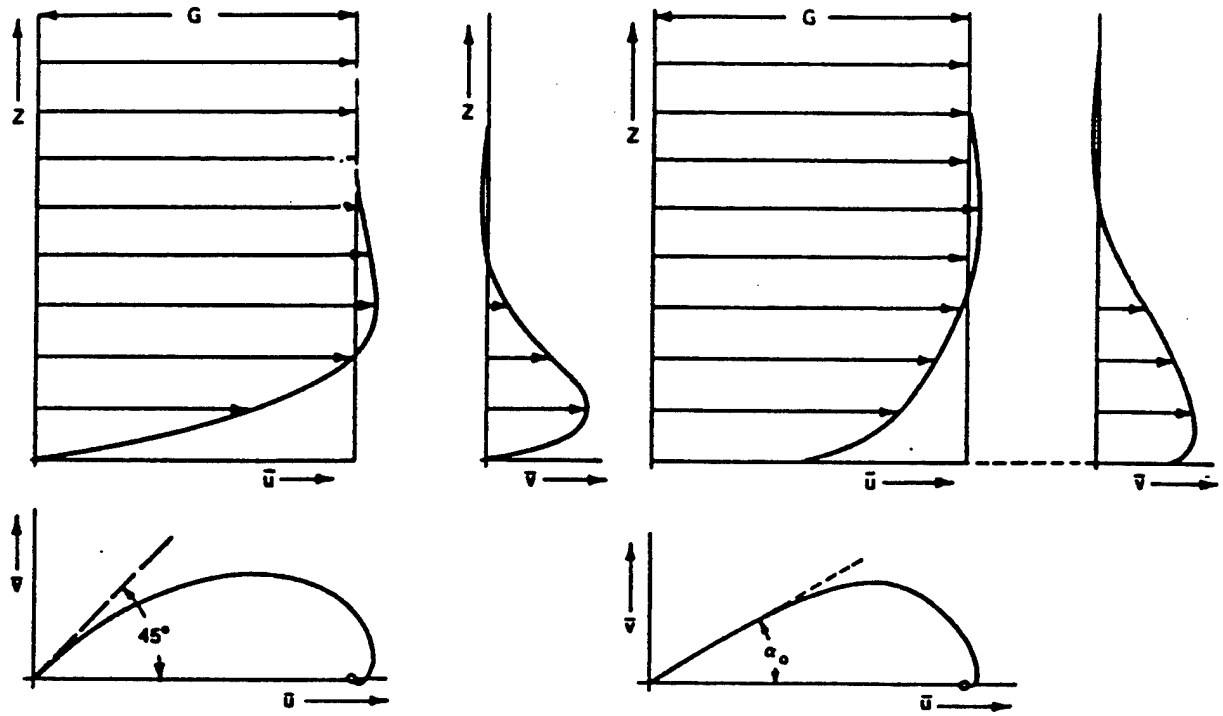

(a) The Ekman spiral in laminar flow, exact solution.
(b) Typical example of the Ekman spiral in turbulent flow (from Prandtl, 1965)

Figure 14. Ekman Spiral for Horizontal Wind in ABL (from: Plate, 1971)

To recapitulate, the ABL is a region of the atmosphere characterized by the interaction of the geostrophic wind (v_g or $G = |v_g|$,) and the Coriolis force (f); its thickness is h and turbulent momentum transfer is characterized by an effective eddy diffusivity K. Reference to Fig.5 above and to the discussion at the end of Section 2.3 shows that the effective eddy diffusivity parameter K is not a constant but increases with spatial scale. Representative values of the mixing height h_d as a function of latitude and of eddy diffusivity are listed in Table 9.

The above suggests that near the equator where the Coriolis factor f is almost zero and the mixing depth h_d is very large, the mixed region or ABL can encompass most of the troposphere.

Table 9. The Mixing Height h_d at Different Latitudes

Latitude ϕ (deg)	0	2	20
Coriolis factor f (sec^{-1})	0	0.05	0.5
• If $K = 10^2$ m^2/sec,[a] h_d(m)	∞	200	63
• If $K = 10^4$ m^2/sec,[b] h_d(m)	∞	2,000	630

[a] From Fig. 5, $\sigma_y \sim 100$ m.

[b] From Fig. 5, $\sigma_y \sim 10$ m.

Clearly, the analysis presented above for Eq. (18) cannot apply down to the surface of the Earth, because there are (or may be) two distinct regimes, namely a viscous sublayer and a surface layer characterized by a constant value of Reynolds stress, rather than by the ansatz of Eq. (15).[26] This surface layer is characterized by the Reynolds stress and also by a parameter z_o specific to the roughness or irregularities of the surface, rather than by values of G and f.

3.4 WIND PROFILE NEAR THE GROUND

In the surface layer, instead of the ansatz (12) for the Reynolds stress terms, we have

$$\tau_{xz} + \nu \, \partial v_1/\partial z \sim u_*^2 \qquad (19a)$$

$$\tau_{yz} + \nu \, \partial v_1/\partial z \sim 0 \quad , \qquad (19b)$$

where $\nu = \mu/\rho$ = kinematic viscosity (which is always very small compared to K, typically $\sim 10^{-1}$ cm^2/sec), while $u_* \sim G/20$. The thickness of this layer is of the order 50 m, and in it the velocity profile is

$$v_1(z) = (u_*/k) \ln (z/z_o) \quad , \qquad (20)$$

where $k \sim 0.4$ is the so-called von Karman constant, and representative values of z_o over land are given in Table 5; over water the values of z_o depend very much on the nature of the sea state (see, in particular, Roll, 1965).

The wind profile of Eq. (20) is somewhat inconvenient for analysis, and for a turbulent boundary layer it is possible to use the empirical profile

---

[26] See Sections 2.4 and 2.5.

$$u/u_h = (z/h)^{1/n} \qquad (21)$$

(cf. Plate, 1971) where h = height of ABL, u_h = velocity at outer edge of the boundary layer (i.e., the geostrophic velocity v_g) and 1/n is a parameter which depends on the roughness, or for a smooth boundary of the flow. The profile of Eq. (21) is clearly more convenient for modeling than any of the other profiles listed. Figure 11 in the discussion of Section 2.4 gives a schematic description of how the wind profile changes with variations in the underlying surface and also for different values of atmospheric stability.

3.5 THE ABL NEAR THE EQUATOR

Reference to Section 3.2 shows that the analysis of the geostrophic wind of Eq. (2) and of (quasi-) geostrophic flow in general breaks down near the equator where the Coriolis factor f is very small (see McIlveen, 1992, pp. 195–207, and Table 8). At low latitudes ($\phi < 5$–$10°$) the geostrophic wind is no longer important and convection goes through the whole of the troposphere rather than being confined to the ABL [see, for instance, Eq. (17) and Table 9, which gives the height of the ABL, $h_d \sim h \sim f^{-1/2}$; the height becomes very large as f tends to zero]. Indeed, at low latitudes centrifugal (Coriolis) forces balance the pressure gradient while at high latitudes friction balances the pressure gradient. This is why there are hurricanes in the tropics vs. ordinary cyclones at higher latitudes.[27]

[27] I wish to thank Frank Gifford for pointing this out to me.

4.0 IN CLOSING

Table 10 supplements Fig. 1 by characterizing the various regions of the atmosphere in terms of:

1. Altitude range
2. Fraction of total atmospheric mass
3. Residence time for an inert tracer
4. Mixing mechanisms.

For the record, I attach Fig. 15 on atmospheric residence times. This is an old figure, presented here largely to indicate the range of variability of the residence times.[28]

It is appropriate to close by referring to some more detailed but readable sources of information:

- McIlveen (1992) provides a careful, detailed, and largely qualitative survey of the physical problems discussed here.
- Three articles that look useful for the non-specialist (i.e., more than monographs on the Atmospheric Boundary Layer and on Atmospheric Turbulence) are found in the Second (1992) Edition of the *Encyclopedia of Physical Science and Technology*, R.A. Meyers, Ed., Academic Press, are those by Panofsky, Schnelle, and Stull.

The ABL is at present still a topic of active research, so the concepts and notations are changing. Note that standard meteorology texts of the 1960's and 1970's may not even include the terms "Atmospheric Boundary Layer" (or "Planetary Boundary Layer") in the index.

---

[28] The sources listed there are cited in Reiter and Bauer, 1975.

Table 10. Atmospheric Altitude Regimes

Atmospheric Region	Altitude Range	Fraction of Total Mass	Typical Residence Time	Mechanism for Mixing
Surface Layer (ASL)	< 50–100 m	.009	3 hrs	Mechanical effects due to near-surface wind gradient, etc.
Boundary Layer (ABL)	0.1–1 km	0.07	24 hrs	Thermal effects: day/night surface temperature variation leading to inversion—stable at night, unstable in daytime (i.e., 24-hour turnover).
Free Troposphere	1–11 km	0.7	30 days	Synoptic-scale turbulence due to interaction of frontal systems (i.e., potential temperature and humidity changes varying on a scale of perhaps 12 hours and some hundreds of km).
Stratosphere	11–50 km	0.23	1 yr	"Blini": flat layers of turbulence (~100 m thick) due to wind shears embedded in a not-very-turbulent environment.
Mesosphere	50–85 km	6×10^{-4}	> 1 yr	"Breaking" of acoustic-gravity waves.
Thermosphere	> 85 km	7×10^{-6}	> 1 yr	Molecular mixing and some plasma effects.

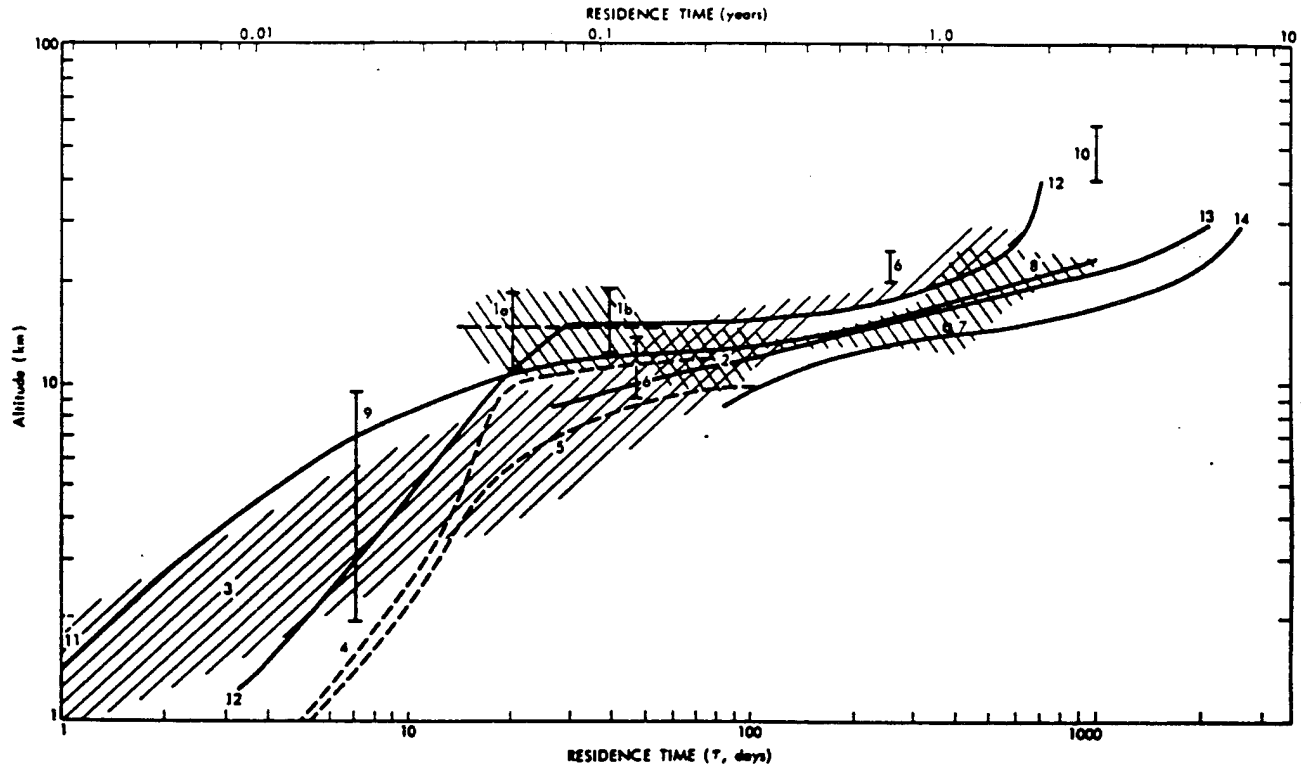

(1) After Reiter et al. (1975) from $^{32}P/^{7}Be$ ratios, subject to cyclonic bias; (a) Median value for fall, (b) Median value for spring, each assuming a transition time through the troposphere of 3 days. (2) Residence times of O_3 entering the troposphere. (3) Estimated residence times for winter, including latitudinal variability. (4) HTO residence times in troposphere according to Ehhalt (1973). (5) Tropospheric aerosol residence times according to Machta et al. (1970). (6) Residence times assumed in box model by Krey and Krajewski (1970) to predict nuclear debris fallout. (7) From ^{14}C distributions, according to Johnston (1974); includes import from higher levels; residence time, therefore, appears high. (8) Residence time (including tropospheric residence time assumed to be 20 days) according to model by Fabian (1974) and Fabian and Libby (1974) which is based upon e-folding depletion of an injection in a certain altitude region over the entire latitude range. (9) Residence times of aerosols in west-central United States from ^{210}Pb concentrations (Moore et al., 1973). (10) Injections at 40-60 km (Leipunskii et al., 1970). (11) From diffusion coefficients according to Chang et al. (1073). (12) From diffusion coefficients according to McElroy et al. (1974). (13) One-dimensional model of Chang, personal conversation, 1974. (14) One-dimensional model of Hunten, personal conversation, 1974.

Figure 15. Atmospheric Residence Time vs. Altitude (Source: Reiter and Bauer, 1975)

BIBLIOGRAPHY

Barry, R.G., and R.J. Chorley, *Atmosphere, Weather and Climate*, Methuen, London, 3rd Ed., 1976. (Later revisions are available.)

Bauer, E., "The Growth and Disappearance of Tracer Clouds in the Atmosphere," IDA Note N-890, June 1983.

Berry, F.A., E. Bolay, and N.R. Beers, Eds., *Handbook of Meteorology,* NAVAER 50-18-503 (McGraw-Hill, 1945).

Culkowski, W.M., "Time Exposure Photography of Smoke Plumes," USAEC Report ORO-359, Weather Bureau, Oak Ridge, TN, 1961.

Davenport, A.G., "The Relation of Wind Structure to Wind Loading," National Physical Laboratory Symposium 16, *Wind Effects on Buildings and Structures*, pp. 54–102, 1965.

Dion, D., and B. Leclerc, "Investigation of the Air Refractivity Effects on IR Sensors in the Marine Boundary Layer," DREV Report 4570/90, August 1990.

Doty, S.R., et al., "A Climatological Analysis of Pasquill Stability Categories based on STAR Summaries," NOAA/EDS, April 1976.

Dritschl, D.G., and B. Legras, "Modeling Oceanic and Atmospheric Vortices," *Phys. Today*, p. 44, March 1993.

Geiger, R., *The Climate Near the Ground*, Harvard University Press, 1965.

Gossard, E.E., and W.H. Hook, *Waves in the Atmosphere*, Elsevier, Amsterdam, 1975.

Hage, K.D., "Particle Fallout and Dispersion Below 30 km in the Atmosphere," Travelers Research Center, Report SC-DC-64-1463, prepared for Sandia Corp., available from NTIS, 1964.

Headley, R.M., Jr., and W. Trahan, "Report on IR Refraction and Mirages: Analysis of Test Data Collected with IR Propagation Sensor (IRP) and Horizon IR Surveillance Sensor (HISS)," NSWC Memo, 11 October 1994, presented at 1995 IRIS-TBD Conference.

Hobbs, P.V., "Scales Involved in the Formation and Organization of Clouds and Precipitation," in *Clouds—Their Formation, Optical Properties and Effects*, P.V. Hobbs and A. Deepak, Eds., Academic Press, 1981.

List, R.J., Compiler, *Smithsonian Meteorological Tables*, 6th Ed., 1984.

McIlveen, R., *Fundamentals of Weather and Climate*, Chapman & Hall, London, 1992.

Minnaert, M, "Light and Color in the Outdoors," Springer, New York, 1993 (translated from Dutch edition of 1974).

Mokhov, I.I., and M.E. Schlesinger, "Analysis of Global Cloudiness – 2. Comparison of Ground-Based and Satellite-Based Cloud Climatologies," *J. Geophys. Res.* **99** (D8), 17045, 20 August 1994.

Monin, A.S., "The Atmospheric Boundary Layer," *Ann. Revs. of Fluid Mech.* **2**, 225, 1970.

Munn, R.E., *Descriptive Micrometeorology*, Academic Press, 1966. (Hickman, 1963.)

Nuclear Regulatory Commission, "Proposed Revision 1 to Regulatory Guide 1.23—Meteorological Programs in Support of Nuclear Power Plants" (see in particular Tables 1 and 3), December 1980.

Oke, T.R., *Boundary Layer Climates*, Methuen, London, 1978.

Panofsky, H.A., "The Atmospheric Boundary Layer Below 150 Meters," *Ann. Revs. of Fluid Mech.* **6**, 147, 1974.

Panofsky, H.A., "Atmospheric Turbulence," p. 297 ff. in R.A. Meyers, Ed., "Encyclopedia of Physical Science and Technology," Academic Press, Second Edition, 1992, Vol. 2.

Panofsky, H.A., and J.A. Dutton, "Atmospheric Turbulence," Wiley-Interscience, 1984. (A good book which is out of print.)

Pasquill, F., and F.B. Smith, *Atmospheric Diffusion*, Third Edition, Horwood Halsted Press, New York, 1983.

Plate, E.J., "Aerodynamic Characteristics of Atmospheric Boundary Layers," DOE Critical Review Series TID-25465, 1971.

Ramage, C.S., "Prospects for Weather Forecasting," *Bull. Amer. Meteor. Soc.* **57**, 4, 1976.

Reiter, E.R., and E. Bauer, "Residence Times of Atmospheric Pollutants," p. 2-125 ff. in *The Natural Stratosphere of 1974*, CIAP Monograph 1, Document PB-246 318, 1975.

Roll, H.U., *Physics of the Marine Atmosphere*, Academic Press, 1965.

Schnelle, K.B., "Atmospheric Dispersion Modeling," in R.A. Meyers, Ed., *Encyclopedia of Physical Science and Technology*, Academic Press, Second Edition, 1992, Vol. 2. (This is a concise summary of the NOAA/EPA dispersion model.)

Slade, D.H., Ed., *Meteorology and Atomic Energy*, Department of Energy, 1968.

Smith, F.B., "Low-Wind-Speed Meteorology," *Met. Magazine*, **121**, 141, 1992.

Stull, R.B., "Atmospheric Boundary Layer," p. 237 ff. in R.A. Meyers, Ed., Encyclopedia of Physical Science and Technology, Academic Press, Second Edition, 1992, Vol. 2. (I find this much better than Stull's Monograph *An Introduction to Boundary Layer Meteorology*, Kluwer Academic, 1988.)

Sutton, O.G., *Atmospheric Turbulence*, Methuen, London, 2nd Ed., 1955.

Sykes, R.I., "The SCIPUFF-PC Code," ARAP Draft Report, 1994.

Tennekes, H., "The Atmospheric Boundary Layer," *Physics Today*, **27**, 52, 1974.

Tennekes, H., and J.L. Lumley, *A First Course in Turbulence*, MIT Press; see especially p. 166 ff., 1972

Trahan, J.W., "Infrared Refraction and Mirages," Presented at 1995 IRIS-TBD Conference, Vol. I, p. 185, July 1995.

Turner, D.B., *Workbook of Atmospheric Dispersion Estimates*, USEPA, revised, 1970.

Tverskoi, P.N, Physics of the Atmosphere, "A Course in Meteorology," Israel Program for Scientific Translations, 1965 (approx.).

U.S. Forest Service, *Southern Forestry Smoke Management Guidebook*, USDA Forest Service General Technical Report SE-10, December 1976.

Valley, S.L., Ed., *Handbook of Geophysics and Space Environments*, USAF, McGraw-Hill, 1965.

APPENDIX A

ATMOSPHERIC STABILITY

APPENDIX A
ATMOSPHERIC STABILITY

A.1 FORMAL DISCUSSION OF LAPSE RATE

The purpose of this Appendix is to expand on the discussion of Section 2.3 with a more detailed review of the conditions for atmospheric stability that are relevant to transport in the ABL. Specifically, we relate the conditions for atmospheric stability by comparing the vertical gradient of the temperature, $\partial T/\partial z$, and of the potential temperature, $\partial\theta/\partial z$, to the gradients that would apply in an adiabatic transformation of an air parcel. An adiabatic transformation is one in which the designated air parcel neither gains nor loses energy; if the transformation is reversible (i.e., it takes place quasi-statically), then it is isentropic.

Consider the vertical atmospheric motion in the absence of horizontal winds. For an ideal gas, the equation of state is

$$p/\rho = RT \tag{A.1}$$

where R is the gas constant per gram, not per mole, and thus the first law of thermodynamics implies

$$dQ = c_p\, dT - RT\, d\rho/\rho \tag{A.2}$$

where Q = enthalpy

c_p = specific heat at constant pressure.

For adiabatic motion,

$$dQ = 0 \tag{A.3}$$

and thus[1]

$$(\partial T/\partial p)_{ad} = RT/c_p\, p \quad . \tag{A.4}$$

---

[1] This is the traditional definition of an adiabatic process in meteorology [i.e., constant enthalpy ($c_p\, \Delta T$) rather than constant entropy]. It is assumed that the pressure of the air parcel is the same as that of the ambient atmosphere; if the process is reversible, then entropy is conserved also.

Now, the basic equation for vertical motion in the absence of flow is

$$\partial p/\partial z = -g\rho \quad . \tag{A.5}$$

Thus, for an ideal gas, the rate of change of temperature with altitude along an adiabatic path is the *adiabatic lapse rate* – γ_{ad}[2]

$$(\partial T/\partial z)_{ad} = -g/c_p = -\gamma_d = -9.8\ ^\circ C/km \text{ for dry air} \tag{A.6a}$$

$$-\gamma_s = -6.5\ ^\circ C/km \text{ for wet (saturated) air} \quad .[3] \tag{A.6b}$$

In contrast to the adiabatic lapse rate γ_{ad}, with its particular limits for dry and saturated air, the ambient temperature gradient $\partial T/\partial z = -\gamma$ is referred to in meteorological usage as the *lapse rate.*

A.2 BEHAVIOR OF AIR PARCELS FOR DIFFERENT STABILITY

Now let us sketch the behavior of parcels of air in the troposphere for different values of $\partial T/\partial z = -\gamma$. A "parcel of air" may be regarded as a test sample of air inside an adiabatic balloon (i.e., one which permits rapid pressure equalization but no energy transfer across it). This is a physically useful concept because pressure equalization is fast compared with energy transfer or temperature equalization. It is therefore reasonable to view air parcels as moving along an adiabatic path. In general, $\partial T/\partial z$ is not equal to $(\partial T/\partial z)_{ad}$, and it is the relative magnitude of these two quantities that determines how the test air parcel moves. We distinguish between stable and unstable motions, which are sketched in Figs. A.1a and A.1b, respectively.

Stable Motion

If

$$\partial T/\partial z < (\partial T/\partial z)_{ad} \text{ or } \gamma > \gamma_{ad} \tag{A.7a}$$

then, if one displaces a parcel of air from its initial position along the adiabatic path, its temperature will be higher than that of its surroundings and so its density will be lower than ambient and buoyancy forces it back to its initial position (i.e., its position is stable).

---

2 The sign is conventional (i.e., γ is always positive).

3 At very high temperatures, air holds lots of moisture, so γ_s can be as small as – 4 °C/km; at very low temperatures air holds little moisture, so $\gamma_s \Rightarrow \gamma_d$.

Unstable Motion

Conversely, if

$$\partial T/\partial z > (\partial T/\partial z)_{ad} \text{ or } \gamma < \gamma_{ad} \qquad \text{(A.7b)}$$

so that the temperature falls off "relatively rapidly" with increasing altitude, an air parcel is unstable, it will tend to "run away" from its initial position.

Thus if $\partial T/\partial z$ is smaller/greater than the representative critical value – γ_{ad}, the thermal layering of the atmosphere is stable/unstable, respectively. Further, the more rapidly/less rapidly T falls off with increasing height, the more vertical motion of air is encouraged/ inhibited.

Cumulus clouds are a sign of convection (i.e., of unstable atmospheric conditions).

A.3 VARIOUS IMPORTANT PHYSICAL CONCEPTS

Potential Temperature

It is convenient and conventional to use the potential temperature θ

$$\theta = T(p_o/p)^{R/Cp} = T(p_o/p)^{0.286} \ , \qquad (3)$$

which is conserved in the adiabatic motion of an air parcel, as variable instead of temperature. Now the stability diagram (temperature vs. height or pressure) is much simpler, in that

$$\partial\theta/\partial z = 0 \text{ for neutral stability} \qquad \text{(A.8a)}$$

$$\partial\theta/\partial z < 0 \text{ for unstable conditions} \qquad \text{(A.8b)}$$

$$\partial\theta/\partial z > 0 \text{ for stable conditions} \ . \qquad \text{(A.8c)}$$

See Fig. A.2.

- The *absolute vorticity* $\eta = (\nabla \times v + \phi)$ where v = flow velocity and f is the Coriolis parameter, $2 \pi \Omega \sin \phi$, where ω = rotation rate of the Earth and ϕ is the latitude. [In general, $\nabla \times v$ is a three-dimensional vector; in practice we are only concerned with one component of this vector, that about a vertical axis, the *relative vorticity*, which is added to the (scalar) Coriolis parameter f].
- Another concept that is conserved in the quasi-geostrophic and adiabatic motion of air parcels and which is frequently used in meteorological analyses is the *potential vorticity* PV, which is the product of the *absolute vorticity* η and the *static stability* $(1/\theta)\ \partial\theta/\partial p$:

$$PV = (\eta/\theta)\, \partial\theta/\partial p \quad . \qquad (A.9)$$

The PV is important because in real geophysical flows the global distribution of PV on surfaces of constant entropy largely determines the entire fluid motion (see, e.g., Dritschl and Legras, 1993).

A.4 MORE COMMENTS ON STABILITY CATEGORIES.

In the "old" (World War II) *Handbook of Meteorology*, Berry et al., 1945, it is stated (on p. 792) that stability may be determined instrumentally or visually. I reproduce their characterization of different levels of stability because it offers insight from an era before modern instrumentation was widely available, so that visual observations were more important than they are now, and were conducted more carefully than they tend to be done nowadays.

1. Extreme stability throughout the atmosphere. Poor visibility, haze layers, stratiform clouds only, or no clouds at all.

2. Extreme stability in one layer. One stable layer, such as at the top of a layer of cold-air advection; flat-topped cumulus humilis, haze layer; perhaps altostratus or altocumulus; sometimes stratocumulus cumulogenitus.

3. Slight stability. Haze layers, trade cumulus over the oceans, limited tops to cumulus and often stratocumulus.

4. Slight instability. Good visibility, no haze layer, cumulus congestus and chimney cumulus, cumulonimbus over mountains, occasional light showers.

5. Extreme instability. Organized cumulonimbus system with associated cirrus, altostratus and stratocumulus decks, turbulence, frequent moderate to heavy showers, often with steady light rain between showers.

In the modern context of quantitative characterization of air pollution, one uses a parametric, quantitative characterization of stability in the surface layer to determine the rate of dispersion of pollutant or tracer clouds. Table 3 in Section 2.3 above presents a characterization of atmospheric stability in terms of the 6–7 Pasquill-Gifford stability classes A–F/G. This includes estimates developed by the U.S. Environmental Protection Agency for conditions over land in the United States: these estimates do not necessarily apply over water, or in different geographic regions.

From Table 3 it is clear that some judgment is called for in the assignment of Pasquill-Gifford classes, and indeed Panofsky and Dutton (1984, p. 244), suggest that the Pasquill-Gifford stability classes are misused in that many situations are listed as "neutral"

or D stability, when B or C stability would be more appropriate. Note that most discussions of stability refer to conditions over land; conditions over the oceans—two-thirds of the total surface of the globe—are significantly different.

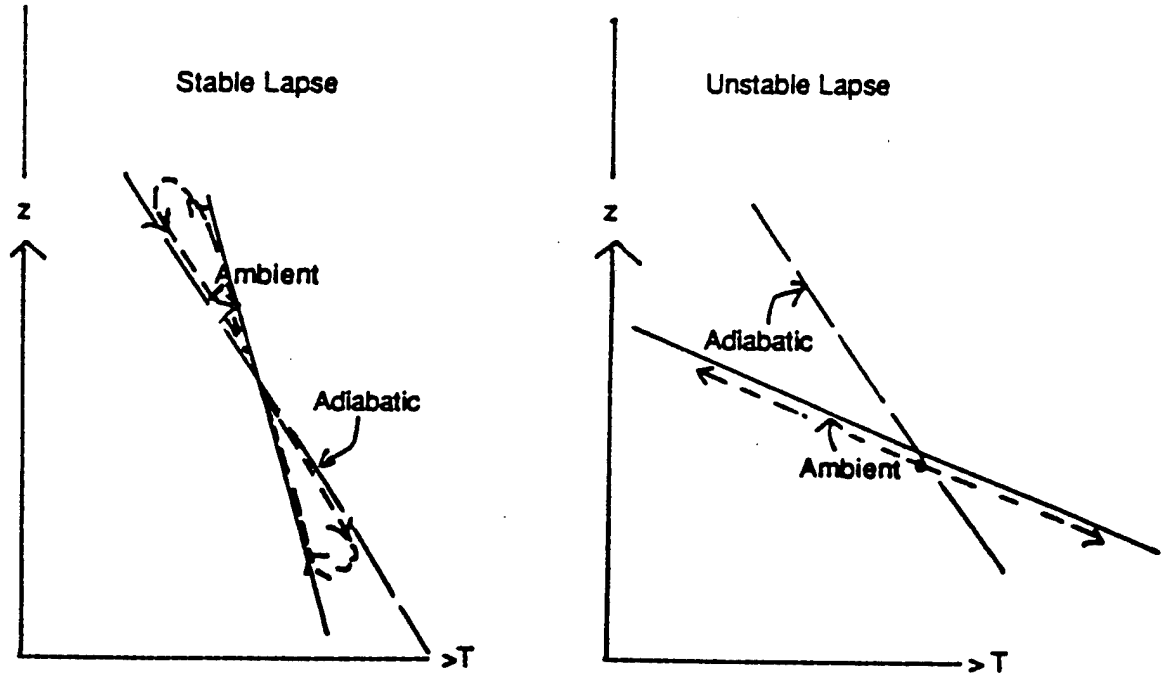

Air parcel returns to its initial location

Air parcel runs away from its initial location

Figure A.1. Stable and Unstable Atmospheric Lapse Rate

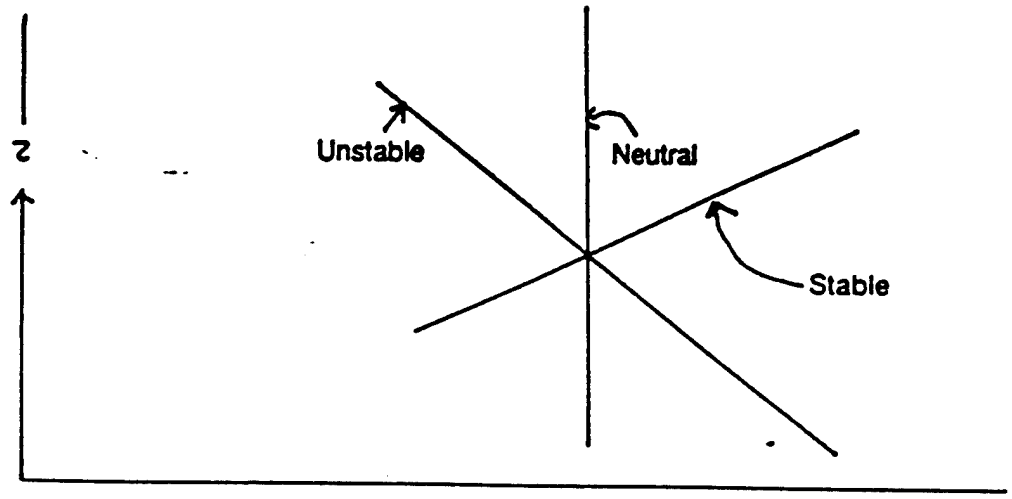

Potential Temperature θ

Figure A.2. Temperature-Height Graph Using Potential Temperature to Illustrate Stability

REPORT DOCUMENTATION PAGE

Form Approved
OMB No. 0704-0188

1. AGENCY USE ONLY *(Leave blank)*	2. REPORT DATE	3. REPORT TYPE AND DATES COVERED
	April 1996	Final—May 1994 to November 1995

4. TITLE AND SUBTITLE
The Lowest Atmosphere: Atmospheric Boundary Layer Including Atmospheric Surface Layer

5. FUNDING NUMBERS
DASW01 94 C 0054
ARPA Assignment A-180

6. AUTHOR(S)
Ernest Bauer

7. PERFORMING ORGANIZATION NAME(S) AND ADDRESS(ES)
Institute for Defense Analyses
1801 N. Beauregard St.
Alexandria, VA 22311-1772

8. PERFORMING ORGANIZATION REPORT NUMBER
IDA Document D-1816

9. SPONSORING/MONITORING AGENCY NAME(S) AND ADDRESS(ES)
Defense Advanced Research Projects Agency
3701 N. Fairfax Drive
Arlingrton, VA 22203-1714

10. SPONSORING/MONITORING AGENCY REPORT NUMBER

11. SUPPLEMENTARY NOTES

12a. DISTRIBUTION/AVAILABILITY STATEMENT
Approved for public release; distribution unlimited.

12b. DISTRIBUTION CODE

13. ABSTRACT ***(Maximum 180 words)***

The Atmospheric Boundary Layer (ABL) is the lowest portion of the Earth's atmosphere which is affected significantly by the properties of the Earth's (land or ocean) surface. The ABL may show a large daily variation in wind, temperature, and stability or turbulence. The ABL is typically 0.5–1 km deep, representing roughly 10 percent of the total mass of the atmosphere. The lowest 10 percent of the ABL, or 50–150 m elevation, is called the Atmospheric Surface Layer (ASL); this is the region we live in, and some of its characteristics are important for a variety of applications. This document provides the basic physics background for applications such as the spreading of tracer clouds in the atmosphere, forest fires, optical refraction near the surface (mirages), etc. It is becoming customary to use the term Atmospheric (vs. Planetary) Boundary Layer (and Surface Layer) to distinguish from the comparable Oceanic Layers. Note that the top of the ABL is normally placed at 0.5–1 km, which is appropriate for mid-latitude conditions. However, at some low-latitude locations, such as the Persian Gulf or central Texas, the top of the ABL frequently reaches 3–4 km in the daytime in summer.

14. SUBJECT TERMS
Earth's atmosphere, lower atmosphere, temperature, atmospheric turbulence, atmospheric stability, atmospheric wind profile

15. NUMBER OF PAGES
65

16. PRICE CODE

17. SECURITY CLASSIFICATION OF REPORT	18. SECURITY CLASSIFICATION OF THIS PAGE	19. SECURITY CLASSIFICATION OF ABSTRACT	20. LIMITATION OF ABSTRACT
UNCLASSIFIED	UNCLASSIFIED	UNCLASSIFIED	SAR